JOURNAL OF VIROLOGY, Oct. 2010, p. 10727–10747 Vol. 84, No. 20
0022-538X/10/$12.00 doi:10.1128/JVI.00122-10

Simian Virus 40 Activates ATR-Δp53 Signaling To Override Cell Cycle and DNA Replication Control[▽]

Gabor Rohaly, Katharina Korf, Silke Dehde, and Irena Dornreiter*

Heinrich-Pette-Institut für Experimentelle Virologie und Immunologie an der Universität Hamburg, Martinistr. 52, D-20251 Hamburg, Germany

Received 19 January 2010/Accepted 22 July 2010

During infection, simian virus 40 (SV40) attempts to take hold of the cell, while the host responds with various defense systems, including the ataxia-telangiectasia mutated/ATM-Rad3 related (ATM/ATR)-mediated DNA damage response pathways. Here we show that upon viral infection, ATR directly activates the p53 isoform Δp53, leading to upregulation of the Cdk inhibitor p21 and downregulation of cyclin A-Cdk2/1 (AK) activity, which force the host to stay in the replicative S phase. Moreover, downregulation of AK activity is a prerequisite for the generation of hypophosphorylated, origin-competent DNA polymerase α-primase (hypo-Polα), which is, unlike AK-phosphorylated Polα (P-Polα), recruited by SV40 large T antigen (T-Ag) to initiate viral DNA replication. Prevention of the downregulation of AK activity by inactivation of ATR-Δp53-p21 signaling significantly reduced the T-Ag-interacting hypo-Polα population and, accordingly, SV40 replication efficiency. Moreover, the ATR-Δp53 pathway facilitates the proteasomal degradation of the 180-kDa catalytic subunit of the non-T-Ag-interacting P-Polα, giving rise to T-Ag-interacting hypo-Polα. Thus, the purpose of activating the ATR-Δp53-p21-mediated intra-S checkpoint is to maintain the host in S phase, an optimal environment for SV40 replication, and to modulate the host DNA replicase, which is indispensable for viral amplification.

Infection of quiescent CV-1 cells with the primate polyomavirus simian virus 40 (SV40) induces cell cycle progression and stimulates host cell DNA replication, which is mandatory for viral amplification. SV40 uses only a single viral protein, T antigen (T-Ag), for its own replication; all other components have to be provided by the host. Initially, a specifically phosphorylated subclass of T-Ag binds to a palindromic sequence in the SV40 origin (43), and in the presence of ATP, T-Ag forms a double-hexamer nucleoprotein complex leading to structural distortion and unwinding of origin DNA sequences (5). In concert with the cellular single-strand DNA binding protein RPA and topoisomerase I, the DNA helicase activity of T-Ag promotes more-extensive origin unwinding, forming a preinitiation complex (pre-RC), resulting in an initiation complex (53). Once the initiation complex forms, the primase activity of the heterotetrameric DNA polymerase α-primase (Polα) complex, consisting of the p180 catalytic subunit, the p70 regulatory subunit, and the p48/58 primase subunits, synthesizes a short RNA primer on each template strand, which is extended by the DNA polymerase activity of Polα (6, 17). Immediately after the first nascent RNA/DNA primer is synthesized, the complete replication machinery is assembled, and elongation at both forks by the processive DNA polymerase δ ensues (62). Thus, during the initiation of SV40 replication, T-Ag performs many of the functions attributed to the eukaryotic pre-RC complex proteins, including Orc, Cdc6, Cdt1, and kinase-independent cyclin E, which facilitates loading of the putative replication helicase Mcm2-7 onto the eukaryotic origin (4, 18). Biochemical evidence shows that initiation of SV40 and eukaryotic DNA replication occurs by the physical interaction of Polα with the appropriate pre-RC in the immediate vicinity of the origin. In SV40, Polα is loaded onto the origin by direct physical contact between the helicase T-Ag and its p180 N-terminal domain C (14, 15, 16). In eukaryotes, Cdc45, Mcm10, and And-1 cooperate to recruit Polα to the origin-initiation complex, thereby tethering the replicase to the origin-loaded Mcm2-7 helicase (34, 61).

Although SV40 and chromosomal DNA replication share the same essential replication factors that are recruited to the appropriate pre-RC, there are noticeable differences between the SV40 and eukaryotic replication systems. The viral system allows unregulated multiple firing of the origin, whereas in the eukaryotic system, origin-dependent initiation of replication is regulated and restricted to firing only once per cell cycle. Reinitiation at origins within a cell cycle is prevented by the inactivation of pre-RC components in S and G_2. The cyclin-dependent kinases (Cdks) play a central role in establishing a block to rereplication through phosphorylation of each of the components. At present, several proteins of the mammalian pre-RC, such as Orc1, Cdt1, Cdc6, and the Mcm complex are phosphorylated by cyclin A (cycA)-Cdk2/1 (AK) and, as a result, are degraded or inactivated (1, 26, 30, 33, 40). Nevertheless, not all of the pre-RC components mentioned above are utilized by SV40, and accordingly, not all are involved in viral initiation control. However, in both replication systems, DNA synthesis is initiated by Polα and its initiation activity is regulated by Cdks (55). Moreover, AK-phosphorylated Polα is not recruited to mammalian origins *in vivo* (13) and is unable to initiate SV40 replication *in vitro* (47, 57, 58). Considering that cellular mechanisms blocking the rereplication of DNA

* Corresponding author. Mailing address: Heinrich-Pette-Institut für Experimentelle Virologie und Immunologie, Martinistr. 52, D-20251 Hamburg, Germany. Phone: 49-40-48051-224. Fax: 49-40-48051-222. E-mail: irene.dornreiter@hpi.uni-hamburg.de.

▽ Published ahead of print on 4 August 2010.

act by AK phosphorylation of the replication factors mentioned above, especially Polα, it is feasible to suggest that downregulation or even inhibition of this kinase activity promotes dysregulation of replication control in SV40-infected cells.

One pathway that leads to downregulation of AK activity in response to cellular stress is the intra-S checkpoint, which employs the novel p53 isoform Δp53 (45). In UV-damaged S-phase cells, ATR (ataxia-telangiectasia mutated [ATM]-Rad3 related)-activated Δp53 upregulates the Cdk inhibitor p21, resulting in a transient reduction in AK activity and decelerated S-phase progression (45). Here we demonstrate that SV40 lytic infection triggers the ATR signaling cascade, leading to the activation of Δp53 and accordingly a p21-mediated drop in AK activity to prevent AK-catalyzed inactivation of the hypophosphorylated, T-Ag-interacting Polα (hypo-Polα) subclass, which is essential for the initiation of viral DNA replication.

MATERIALS AND METHODS

Cell culture, synchronization, treatment, and SV40 infection. The following cell lines were grown according to the supplier's instructions: CV-1 (African green monkey epithelial kidney cell line; ATCC CCL70), H1299 (human lung carcinoma; ATCC CLR-5803), and High 5 (*Trichoplusia ni* egg cells; Invitrogen). Doxycycline (Dox)-inducible TO-CV-1-TR (empty vector, encoding the tetracycline repressor [TR] only), TO-CV-1, and TO-H1299 cell lines were cultured as described previously (45). Hybridomas SJK132-20 (56), HP180-12 (13) (Polα p180 subunit specific), and PAb101 (T-Ag specific) (21) were grown as spinner cultures in RPMI 1640–Dulbecco's modified Eagle's medium (DMEM) (1:1) supplemented with 5% fetal calf serum (FCS) and 2 mM glutamine at 37°C. Cells were γ-irradiated (10 Gy) using a ^{137}Cs source or were UV irradiated (10 J/m^2; Stratagene Stratalinker). Cells were arrested in pseudo-G_0 by incubation with isoleucine-depleted DMEM plus 5% FCS, and cell cycle progression was monitored by fluorescence-activated cell sorting (FACS) as described previously (13). CV-1, TO-CV-1-TR, and TO-CV-1 cells were inoculated with wild-type SV40 (strain 776; ATTC 45019) at an input multiplicity of infection (MOI) of 10. After an adsorption period of 1.5 h at 37°C, unabsorbed virus was replaced with fresh, warm supplemented DMEM, and the infected cells were further incubated until harvest. SV40-infected TO-CV-1 cells were induced with Dox (1 μg/ml) at 1.5 h postinfection (hpi). For ATM inactivation, the compound KU-55933 (10 μmol/liter; Calbiochem) was added at 1.5 and 24 hpi. Caffeine (Sigma) was added to the culture medium (final concentration, 5 mM) at 1.5 hpi. Infected CV-1 cells were treated with 10 μM MG132 (Calbiochem) at 16 hpi for 8 h.

Establishment of inducible TO-CV-1-shRNAp21 cell lines. Short hairpin RNA (shRNA) targeted to human p21 (CGAUGGAACUUCGACUUUGUU) was cloned into the Block-iT tetracycline-inducible H1 RNA interference (RNAi) entry vector pENTR/H1/TO (Invitrogen) according to the manufacturer's protocol, and the resulting construct was confirmed by sequence analysis. CV-1 cells were cotransfected with the pcDNA6/TR and pENTR/H1/TO-shp21 vectors. Blasticidin- and Zeocin-resistant clones were selected after 2 weeks. More than 100 clones were isolated and characterized. UV-irradiated cell clones, designated TO-CV-1-shRNAp21, that are able to downregulate endogenous p21 in the presence of Dox (1 μg/ml) were used in the experiments.

Recombinant adenovirus and infection. Adenoviral (Ad) shRNA DNA was generated by using the Block-iT adenoviral RNAi expression system (Invitrogen) according to the manufacturer's protocol. In brief, double-stranded (ds) oligonucleotides targeting p53 but not Δp53 (GAAGACTCCAGTGGTAATCT) were cloned into the tetracycline-inducible pENTR/H1/TO entry vector. Adenoviral expression clones were created by performing an LR recombination reaction between the pENTR-shRNA construct and the pAd/Block-iT-DEST vector, and the resulting construct, pAd/Block-iT-shRNAp53, was transfected into the HEK-293A producer cell line. TO-CV-1-TR and TO-CV-1-Flag-wtΔp53 cells were exposed to adenovirus Ad-TO-shRNAp53 at an input MOI of 10. Three days after adenovirus infection, cells were Dox (1 μg/ml) induced, and after 2 additional days, they were infected with SV40. Dox was renewed daily.

Fluorescence immunostaining. Cells were grown on coverslips. They either were induced with Dox or were first infected with SV40 and then induced with Dox 1.5 h later. Then they were fixed with 4% paraformaldehyde in phosphate-buffered saline (PBS) for 10 min, permeabilized with 0.5% Triton X-100, washed with PBS, and stored at 4°C. For preextraction, the protocol of Pombo et al. (42) was adapted. In brief, cells were washed with ice-cold PBS followed by ice-cold buffer PB (100 mM potassium acetate [KAc], 30 mM KCl, 10 mM Na_2HPO_4, 1 mM $MgCl_2$, 1 mM dithiothreitol [DTT]), pH 7.4. Soluble proteins were preextracted on ice for 5 min with PB-T (PB containing 0.05% Triton X-100 and Halt protease inhibitor cocktail [1:100] [Thermo Scientific]). After a wash with PB, cells were fixed as described above and were stored in PBS at 4°C. Before fluorescence immunostaining, cells were incubated with 3% bovine serum albumin (BSA)-PBS at 4°C for at least 1 day. The samples were incubated with primary antibodies for 1 h at room temperature, washed with PBS, and then incubated with secondary antibodies for 30 min at room temperature. For nuclear staining, cells were incubated with 4 μg/ml Hoechst stain (Sigma) for 5 min. The primary antibody dilution for rabbit anti-T-Ag R9 was 1:700. Mouse monoclonal M2 anti-Flag, HP180-12 anti-human p180, and SJK132-20 anti-human p180 antibodies were diluted 1:2,000, 1:2, and 1:2, respectively. Alexa Fluor 488-conjugated anti-rabbit and Alexa Fluor 555-conjugated anti-mouse secondary antibodies (Invitrogen) were diluted 1:800. All antibodies were diluted in 3% BSA-PBS. Coverslips were mounted in Mowiol (Calbiochem). For the detection of DNA replication, cells were incubated at 37°C with 10 μM 5-ethynyl-2′-deoxyuridine (EdU) 30 min before preextraction (46). EdU incorporation was visualized using Click-iT EdU AF647 (Invitrogen).

Microscopy. Preextracted samples were scanned with a Zeiss 510 Meta confocal laser-scanning microscope equipped with 3 lasers giving excitation lines at 633, 543, and 488 nm. A Hoechst channel was obtained by nonconfocal scanning with HBO 100 illumination. Data from the channels were collected sequentially with appropriate band-pass filters built into the instrument at a resolution of 512 by 512 pixels, fulfilling the Nyquist criterion. A Zeiss Axiovert 200 microscope with a 63× oil immersion objective (numerical aperture, 1.40) was used. Data sets were processed by Zeiss Advanced Imaging Microscopy (AIM) software, version 3.2, and were then exported to Adobe Photoshop.

ChIP-PCR. A chromatin immunoprecipitation (ChIP)-PCR assay was performed to determine the levels of p53- and Δp53-associated *p21*, *14-3-3σ*, *mdm2*, *bax*, and *PIG3* promoter DNAs as described previously (45).

Quantification of viral DNA synthesis. At specific hours postinfection, cells were labeled with [*methyl*-^{3}H]thymidine (Hartmann Analytic) (30 μCi/ml/10^6 cells) for 1 h. Viral DNA was then extracted by the method of Hirt (24). The incorporation of ^{3}H into newly synthesized viral DNA was determined by liquid scintillation counting. Rates of viral DNA replication were expressed as counts per minute per microgram of viral DNA.

Reverse transcription-PCR (RT-PCR) and Northern blotting. Total RNA from SV40-infected CV-1 cells with wild-type p53 (wtp53 CV-1 cells) was isolated at specific hours postinfection by the acid-guanidinium-phenol-chloroform extraction method (10). Reverse transcription reactions were conducted, and PCR products were detected, as described previously (45). For Northern blot analysis, 10 μg of purified RNA was electrophoresed on a denaturing 1.2% agarose gel containing 3% formaldehyde and was transferred to a Hybond-N membrane (Amersham) as suggested by the suppliers. The filter was hybridized with a Polα p180 subunit DNA probe, which was PCR labeled with [α-^{32}P]dCTP (PCR primers for the DNA polymerase α DNA probe, F [5′-TATATGGATC CACCATGGAACTGGAAGTACTACTGCAG-3′] and R [5′-TATATGAATT CAGTTTCCGGATCTCTCTGGC-3′]). Hybridization of the filter and washing procedures were carried out as recommended by the manufacturer.

Generation of phosphospecific antisera. An antiserum against the phosphorylated p180 residue S-209 of the Polα p180 subunit (anti-P-p180-S209) was generated in guinea pigs using the phosphorylated peptide AVPSGKIApSPV SRK. An antiserum against the phosphorylated T-Ag residue S-120 (anti-P-T-Ag-S120) was generated in rabbits using the phosphorylated peptide DEATAD pSQHSTPPKK. Phosphospecific antibodies against p180 and T-Ag were depleted of cross-reactivity with nonphosphorylated forms of proteins by incubation with bacterially expressed glutathione *S*-transferase (GST)-1α and GST-T1, respectively (14, 20).

Immunological reagents. The generation of the chicken polyclonal antibody IDα against the Polα p180 subunit has been described previously (14). The following commercial antibodies were used: anti-p53 monoclonal antibodies DO1 (Oncogene), DO12, and ICA9 (Serotec); the rabbit polyclonal anti-p53 antibody SAPU (S238-120; Scottish Antibody Production Unit, Lanarkshire, Scotland); a monoclonal anti-γ-H2AX antibody (JBW301); rabbit polyclonal anti-bax and anti-Cdk2 antibodies; a monoclonal anti-mdm2 antibody (SMP14; BD Biosciences); a rabbit polyclonal anti-pig3 antibody (Ab-1); monoclonal anti-cycA (Ab-3) and anti-Ku80 (Ab-1) antibodies (Oncogene); rabbit polyclonal anti-p21 (H-164), anti-cycA (H-432), and anti-14-3-3β (K-19) antibodies; a goat polyclonal anti-14-3-3σ antibody (N-14; Santa Cruz); a monoclonal anti-FLAG

antibody (M2; Sigma); a monoclonal anti-Chk1 antibody (DCS-310; MBL); a rabbit polyclonal anti-TR antibody (TETO1; MoBiTec); rabbit polyclonal anti-phospho-p53-S15 and -S20, -Chk1-S317 and -S345, -Chk2-T68, and -Cdc25C-S216 antibodies (Cell Signaling Technology); a rabbit polyclonal anti-phospho-SMC1-S966 antibody (Bethyl); and a monoclonal anti-phospho-ATM-S1981 antibody (Rockland).

Protein manipulations. Immunoprecipitation, immunoblotting, and far-Western blotting were performed as described previously (13, 14). A chromatin-enriched cellular fraction was isolated as described previously (32) with the following modifications. Cells were lysed in hypotonic buffer (10 mM HEPES [pH 7.9], 10 mM KCl, 1.5 mM $MgCl_2$, 0.34 M sucrose, 10% glycerol, 1 mM dithiothreitol, 5 mM NaF, 1 mM sodium orthovanadate, 0.04% Triton X-100, and Complete protease inhibitor mixture [Roche]) for 10 min on ice. Samples were centrifuged (4 min, 1,300 × *g*, 4°C) in order to separate soluble cytosolic and nucleosolic proteins from chromatin. Chromatin-associated proteins were extracted from the remaining pellet in 100 μl chromatin extraction buffer (50 mM HEPES [pH 7.5], 400 mM NaCl, 5 mM NaF, 1 mM sodium orthovanadate, 1% Triton X-100, 2.5 mM $MgCl_2$) supplemented with 1× protease cocktail inhibitor and 25 U of Benzonase (Novagen) for 30 min on ice and were then centrifuged (10 min, 21,000 × *g*, 4°C).

Expression and purification of recombinant proteins. T-Ag was produced from High 5 cells infected with recombinant baculovirus 941T and was immunoaffinity purified with the anti-T-Ag antibody PAb101 as described previously (16). Recombinant AK2 complexes were generated in High 5 cells and were purified with the suc1 protein as described previously (47). GST fusion proteins were expressed and purified as described previously (14).

Kinase assay. AK2/1 and BK1 activities in CV-1 and SV40-infected CV-1, TO-CV-1-Flag-mutΔp53, -ATR^{kd}, and -shRNAp21 cells were assessed as described previously (45). Purified recombinant AK2 was tested for activity with histone H1 before assaying for kinase activity with 1 μg of p180-GST fusion protein 1α, B, or C as described above.

RESULTS

In SV40-infected CV-1 cells, Δp53 is stabilized but is not complexed to T-Ag. In SV40-infected permissive wild-type *p53* (wtp53) cells, the tumor suppressor p53 is stabilized and forms a complex with virally encoded T-Ag (41). Therefore, we investigated whether the recently discovered p53 isoform Δp53 (45) is also stabilized upon SV40 infection and whether it is then targeted by T-Ag. For the investigation, permissive wtp53 CV-1 cells were infected with SV40, and successful infection was confirmed by monitoring the presence of T-Ag over a period of 72 h at specific hours postinfection by Western blotting (Fig. 1A). Immunoblot analysis using the anti-p53/Δp53 antibody SAPU revealed two reactive proteins that were detectable at 16 hpi. One signal corresponded to a 53-kDa protein and the other to a faster-migrating protein, indicating stabilization of p53 and Δp53 (Fig. 1A). In addition, RT-PCR analysis was performed (45) to monitor the expression of Δp53 at the RNA level in infected CV-1 cells at early and late times postinfection. The data demonstrate that infection of CV-1 cells with SV40 did not modulate the RNA level of the p53 splice variant Δp53 (Fig. 1B). As shown previously, Δp53 contains the N and C termini but lacks residues 257 to 322 from the core domain (45). Therefore, the epitope-specific anti-p53 antibodies DO1 (amino acids [aa] 21 to 25), ICA9 (aa 388 to 393), and DO12 (aa 256 to 270) were used to confirm that the faster-migrating protein is Δp53. Both p53 forms were detected with the N- and C-terminus-specific antibodies (Fig. 1C, DO1 and ICA9), whereas the core-domain-specific antibody detected only p53, not Δp53 (Fig. 1C, DO12), demonstrating that Δp53 is stabilized in infected CV-1 cells.

Subsequently, the ability of Δp53 to interact with T-Ag was investigated by precipitating the viral protein with the anti-T-Ag antibody PAb101 at specific times postinfection. Analysis of T-Ag precipitates with the anti-p53/Δp53 antibody SAPU demonstrated that only p53 was bound to T-Ag (Fig. 1D). In addition, a whole-cell lysate prepared from infected CV-1 cells at 32 hpi was depleted of T-Ag by sequential precipitation with the anti-T-Ag antibody PAb101, and the T-Ag-depleted cell lysate (Fig. 1E, lane 7) was subjected to immunoprecipitation using the anti-p53/Δp53 antibody DO1. Probing of the DO1 precipitate with anti-T-Ag and anti-p53/Δp53 antibodies showed that the depletion of T-Ag also depleted p53 but not Δp53 (Fig. 1E, lane 8), confirming the lack of complex formation between Δp53 and T-Ag. Moreover, immunoblot analysis of the PAb101 and DO1 precipitates with the anti-p53/Δp53 antibody SAPU (Fig. 1E, lanes 1 to 8) verified that Δp53 does not interact with p53 (45).

SV40 induces ATR-mediated phosphorylation and stabilization of Δp53. Since phosphorylation of the N terminus is involved in the stabilization of p53 and Δp53 (45, 49), the phosphorylation statuses of the two N-terminal amino acid phosphate acceptors S-15 and S-20 in infected CV-1 cells were investigated with the respective phosphospecific anti-p53 antibodies. Immunoblot analysis showed significant induction of phosphorylation at S-15 of p53 and Δp53 that was detectable at 16 and 24 hpi, respectively (Fig. 2A). Probing of the membrane with an anti-P-p53-S20 antibody revealed that S-20 was phosphorylated 16 h later than S-15, indicating successive phosphorylation of the N terminus of p53 after SV40 infection. In contrast, Δp53 was not phosphorylated at S-20. This finding is in agreement with previous results demonstrating that phosphorylation at S-20 is abrogated in Δp53 because the Chk1/Chk2 docking site, which is located in the conserved domain V, is deleted (11, 45).

Recently, it was shown that upon UV-induced activation of the intra-S checkpoint, ATR is responsible for phosphorylation at S-15 of Δp53 (45). Thus, the previously described TO-CV-1-Flag-ATR^{kd} cell line was used (45) to investigate whether ATR phosphorylates Δp53 at S-15 in infected cells. Dox-induced expression of ectopic Flag-ATR^{kd} was monitored by immunoblotting (Fig. 2B, Flag-ATR^{kd}), and the effect of dominant-negative ATR^{kd} on the activity of endogenous ATR was evaluated by examining the phosphorylation status of the ATR substrate Chk1 at various times postinfection. In contrast to infected CV-1 cells, where the onset of Chk1 phosphorylation at S-345 and S-317 was noticeable at 16 and 24 hpi, respectively, phosphorylation of these residues was barely detectable in infected ATR^{kd} cells (Fig. 2B, Chk1-S345 and Chk1-S317). In addition, ATM is not impaired in ATR^{kd} cells, as evidenced by the appearance of autophosphorylated ATM and phosphorylated Chk2, H2AX, and T-Ag, all of which were shown to be ATM substrates in SV40-infected cells (48), as well as SMC1 (Fig. 2B). However, inactivation of ATR resulted in extended phosphorylation of ATM and Chk2, suggesting that loss of the ATR/Chk1 pathway prolongs ATM/Chk2-signaling. Evaluation of the phosphorylation statuses of p53 and Δp53 in infected ATR^{kd} cells demonstrated that in contrast to p53, the p53 isoform Δp53 was not phosphorylated at S-15 (Fig. 2C, top). Since ATR-catalyzed phosphorylation at S-15 of Δp53 is a prerequisite for the stabilization of the isoform (45), the impact of nonfunctional ATR on Δp53 stabilization was investigated. Immunoblot analysis showed that the lack of func-

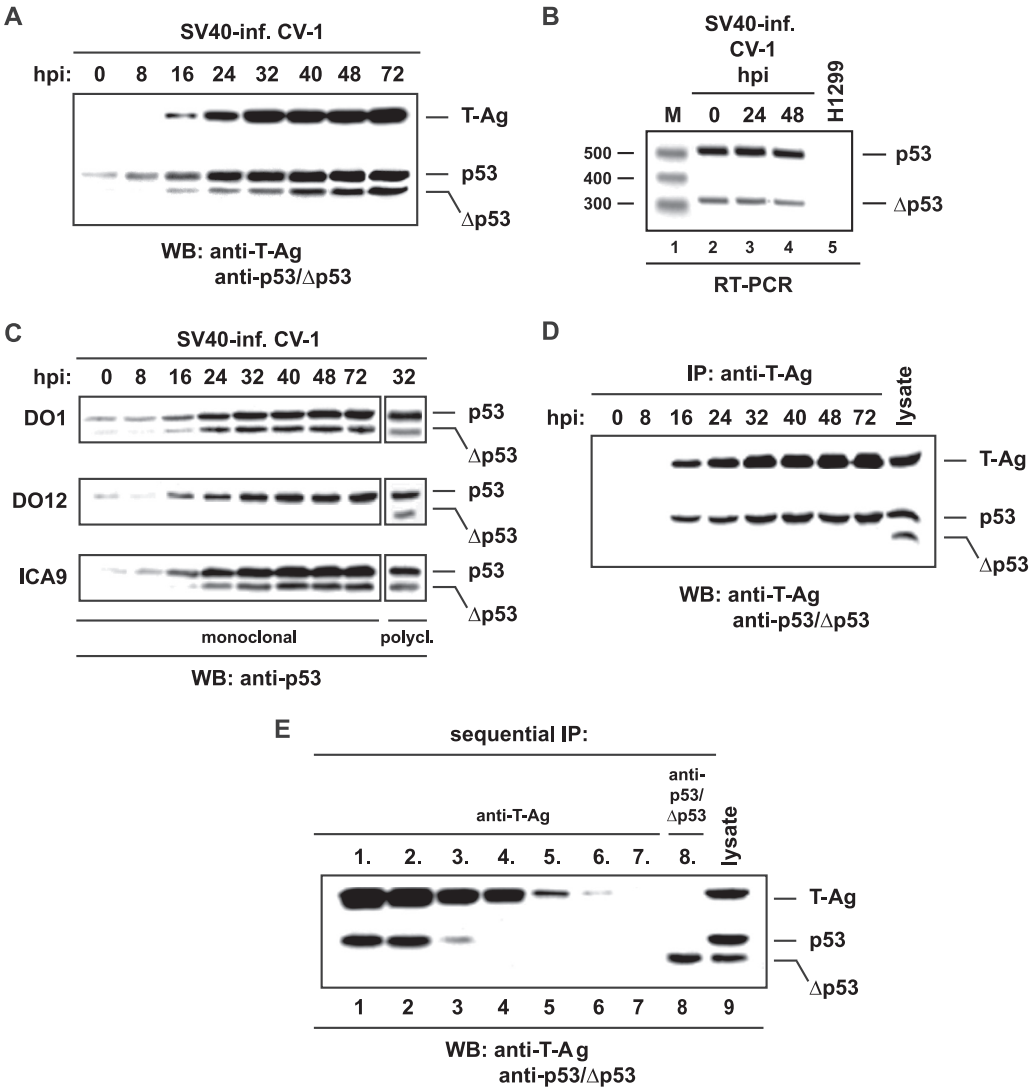

FIG. 1. Δp53 does not interact with T-Ag. (A) Lysates prepared from SV40-infected (inf.) CV-1 cells at the indicated hour postinfection (hpi) were analyzed for T-Ag, p53, and Δp53 expression by immunoblotting (WB) using antibodies PAb101 and DO1, specific for T-Ag and p53/Δp53, respectively. (B) RT-PCR analysis of RNA derived from infected CV-1 cells at different times postinfection (lanes 2 to 4) and from human *p53*-null cells (lane 5). The amplified 520-bp and 325-bp PCR fragments corresponding to p53 and Δp53 are indicated. Lane 1, 100-bp DNA ladder (M). (C) Immunoblot analysis performed with lysates derived from infected CV-1 cells at various times postinfection to analyze p53 and Δp53 expression with the epitope-specific anti-p53 antibodies DO1 (N terminus), ICA9 (C terminus), and DO12 (core domain). Lysates prepared from infected CV-1 cells at 32 hpi were probed with the anti-p53/Δp53 antibody SAPU in order to monitor the expression of p53 and Δp53. (D) PAb101-precipitated T-Ag derived from infected CV-1 cells at various times postinfection was analyzed for complex formation with p53 and Δp53 by use of the anti-p53/Δp53 antibody SAPU. IP, immunoprecipitation. (E) Lysates prepared from infected CV-1 cells at 32 hpi were depleted of T-Ag by sequential precipitation with the anti-T-Ag antibody PAb101 (lanes 1 to 7). A T-Ag-depleted lysate (lane 7) was used for DO1-mediated p53/Δp53 precipitation (lane 8). Anti-T-Ag and anti-p53/Δp53 precipitates were probed with anti-T-Ag antibody R9 and anti-p53/Δp53 antibody SAPU (lanes 1 to 7). A lysate prepared from infected CV-1 cells at 32 hpi served as a positive control (lane 9).

tional ATR prevents robust stabilization of Δp53 but not of p53 (Fig. 2C, bottom). In addition, RNA derived from infected TO-CV-1-Flag-ATR^{kd} cells was analyzed by RT-PCR (45) to rule out the possibility that microRNAs (miRNAs), which were found in SV40 isolates recently (54), negatively affect Δp53 expression in infected ATR^{kd} cells. The data demonstrate that the dominant-negative effect of ectopic Flag-ATR^{kd} did not abrogate the expression of Δ*p53* RNA in uninfected and infected TO-CV-1 cells (Fig. 2D, lanes 2 to 4). This finding was confirmed by treating uninfected and infected CV-1 cells with the ATR/ATM inhibitor caffeine (Fig. 2D, lanes 5 to 7), which also negatively affects the stabilization of Δp53 in UV-irradiated CV-1 cells (45).

The specificity of ATR for Δp53 was further investigated by treating SV40-infected CV-1 and ATR^{kd} cells with the ATM inhibitor KU-55933 (23). Comparative immunoblot analysis with phosphospecific antibodies showed that KU-55933-mediated ATM inactivation inhibited the phosphorylation of Chk2, but not that of Chk1, in CV-1 cells (Fig. 3A, Chk2-T68 and Chk1-S317), whereas in KU-55933-treated ATR^{kd} cells, the

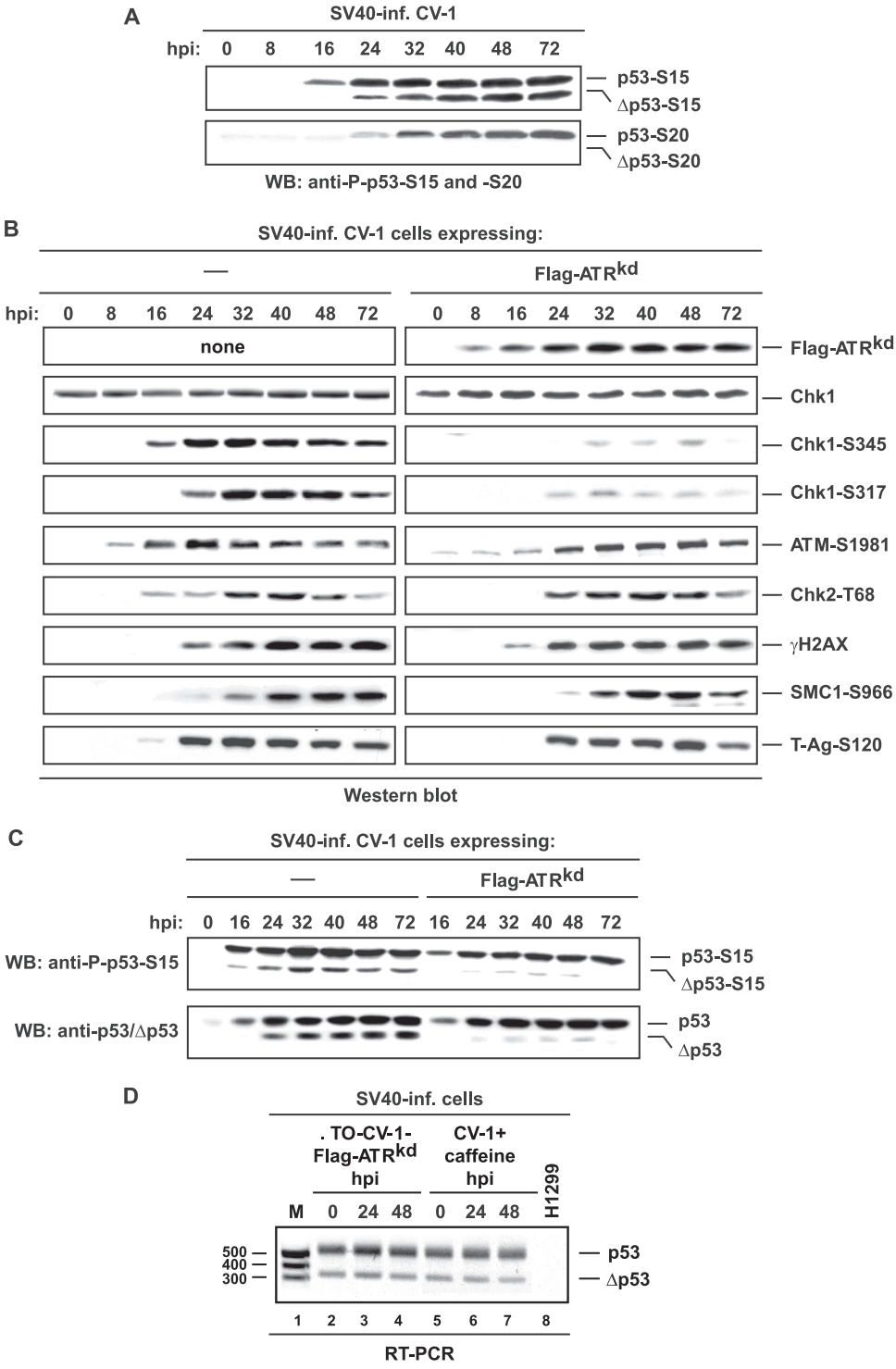

FIG. 2. ATR phosphorylates and stabilizes Δp53. (A) Analysis of phosphorylation of p53 and Δp53 at S-15 and S-20 in infected (inf.) CV-1 cells by immunoblotting (WB) at various times postinfection. (B) Immunoblot analysis of Chk1 expression, S-345 and S-317 phosphorylation of Chk1, and phosphorylation of ATM, Chk2, chromatin-bound H2AX, SMC1, and T-Ag in infected CV-1 and TO-CV-1-Flag-ATR^{kd} cells at various times postinfection. Dox-induced expression of Flag-ATR^{kd} was monitored with anti-Flag antibody M2. (C) Lysates prepared from infected CV-1 and ATR^{kd} cells at various times postinfection were loaded onto the same sodium dodecyl sulfate gel, transferred to the same membrane, and analyzed for S-15 phosphorylation and expression of p53 and Δp53 by comparative immunoblotting. (D) RT-PCR analysis of RNA derived from uninfected (lanes 2 and 5) or infected (lanes 3, 4, 6, and 7) TO-CV-1-ATR^{kd} cells in the absence or presence of caffeine as indicated. Human *p53*-null H1299 cells served as a negative control (lane 8). The amplified 520-bp and 325-bp PCR fragments corresponding to p53 and Δp53 are indicated. Lane M, 100-bp DNA ladder.

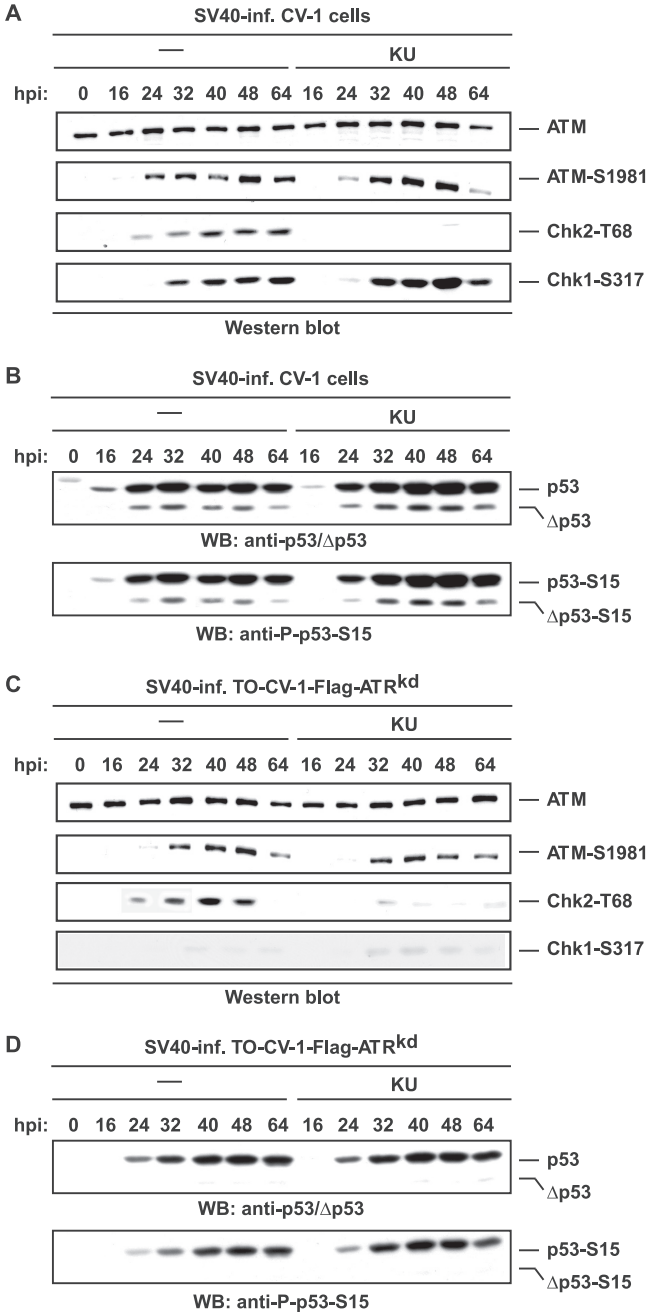

FIG. 3. Stabilization and S-15 phosphorylation of Δp53 depends on ATR but not on ATM. (A) Lysates prepared from infected (inf.) CV-1 cells at various times postinfection in the absence (—) or presence (KU) of KU-55933 were loaded onto the same sodium dodecyl sulfate gel, transferred to the same membrane, and analyzed for ATM expression and S-1981 phosphorylation and for phosphorylation of Chk2 and Chk1 by comparative immunoblotting. (B) Analysis of expression and S-15 phosphorylation of p53 and Δp53 in infected CV-1 cells in the absence or presence of KU-55933, as for panel A. WB, immunoblotting. (C) Comparative immunoblot analysis of infected, Dox-induced TO-CV-1-ATR^{kd} cells as in panel A. (D) Comparative immunoblot analysis of infected, Dox-induced TO-CV-1-ATR^{kd} cells as in panel B.

phosphorylation of both kinases was abolished (Fig. 3C). Interestingly, phosphorylation of the S-1981 autophosphorylation site of ATM still occurred in the presence of KU-55933 in CV-1 cells as well as in ATR^{kd} cells, although in a delayed manner (Fig. 3A and C, ATM-S1981). Stabilization and S-15 phosphorylation, though deferred, were observed for p53 in KU-55933-treated CV-1 and ATR^{kd} cells (Fig. 3B and D), most probably reflecting the fact that in addition to ATM and ATR, SV40 also activates DNA-dependent protein kinase (DNA-PK), a phosphatidylinositol kinase (PIK) kinase (PIKK) that has been shown to phosphorylate p53 at S-15 (27). In contrast, Δp53 was expressed and phosphorylated at S-15 in untreated and KU-55933-treated CV-1 cells (Fig. 3B), but not in ATR^{kd} cells either in the presence or in the absence of KU-55933 (Fig. 3D). Taken together, the data demonstrate that in SV40-infected permissive cells, Δp53 is a substrate for ATR whereas p53 is targeted by various PIKKs.

ATR activates the differential transcriptional activity of Δp53. As shown previously, UV-induced initiation of the intra-S checkpoint leads to ATR-mediated activation of Δp53, resulting in upregulation of the p53-inducible gene products p21 and 14-3-3σ, but not of mdm2, bax, or pig3 (45). Since SV40 infection also induces ATR-mediated phosphorylation and stabilization of Δp53, and since Δp53 is not targeted by T-Ag, it is likely that Δp53 is transcriptionally active. This assumption was first investigated by evaluating the expression level of the p53-inducible gene products mentioned above at specific times postinfection. Increased expression of p21 and 14-3-3σ was detectable at 24 hpi, whereas the mdm2, bax, and pig3 protein levels remained unchanged (Fig. 4A). As expected, all five proteins were upregulated in γ-irradiated CV-1 cells, which served as a positive control (Fig. 4B). It is noteworthy that in γ-irradiated CV-1 cells, upregulation of the antiapoptotic factors p21 and 14-3-3σ preceded p53-induced transactivation of the proapoptotic factors bax and pig3. Chromatin immunoprecipitation (ChIP)-PCR was performed to further assess the effect of Δp53 on the activation of the *p21* and *14-3-3σ* promoters in infected CV-1 cells. In addition, γ-irradiated CV-1 cells were used as a control for the specificity of the ChIP-PCR assay. CV-1 cells were infected or γ-irradiated and were harvested 24 h or 8 h later, respectively. Cross-linked p53/Δp53-DNA complexes were obtained with the N- and C-terminal anti-p53 antibodies DO1 and ICA9, respectively. The core-specific anti-p53 antibody DO12, which recognizes only p53, was used to distinguish between p53 and Δp53. The anti-T-Ag antibody PAb101, which precipitates T-Ag and the T-Ag–p53 complex, served as an additional control. Precipitates obtained from γ-irradiated and infected CV-1 cells were analyzed by immunoblotting either with anti-p53/Δp53 antibodies or with anti-p53/Δp53 plus anti-T-Ag antibodies. Analysis of DO12 and PAb101 precipitates confirmed that Δp53 does not interact with p53, T-Ag, or the T-Ag–p53 complex (Fig. 4C). The presence of precipitated *p21*, *14-3-3σ*, *mdm2*, *bax*, and *PIG3* promoter DNAs was determined by PCR amplification. Endogenous *p21*, *14-3-3σ*, *mdm2*, *bax*, and *PIG3* promoter DNAs were recovered from DO1, ICA9, and DO12 precipitates from γ-irradiated CV-1 cells (Fig. 4D, top). In contrast, ChIP-PCR performed with infected CV-1 cells demonstrated that *p21* and *14-3-3σ* promoter DNAs, but not *mdm2*, *bax*, or *PIG3* promoter DNAs, were retrieved from DO1 and ICA9 precipitates but not from DO12 or PAb101 precipitates (Fig. 4D, bottom). These results demonstrate that in infected CV-1 cells, Δp53 associates with the *p21* and *14-3-3σ* promoters but not with the *mdm2*, *bax*, and *PIG3*

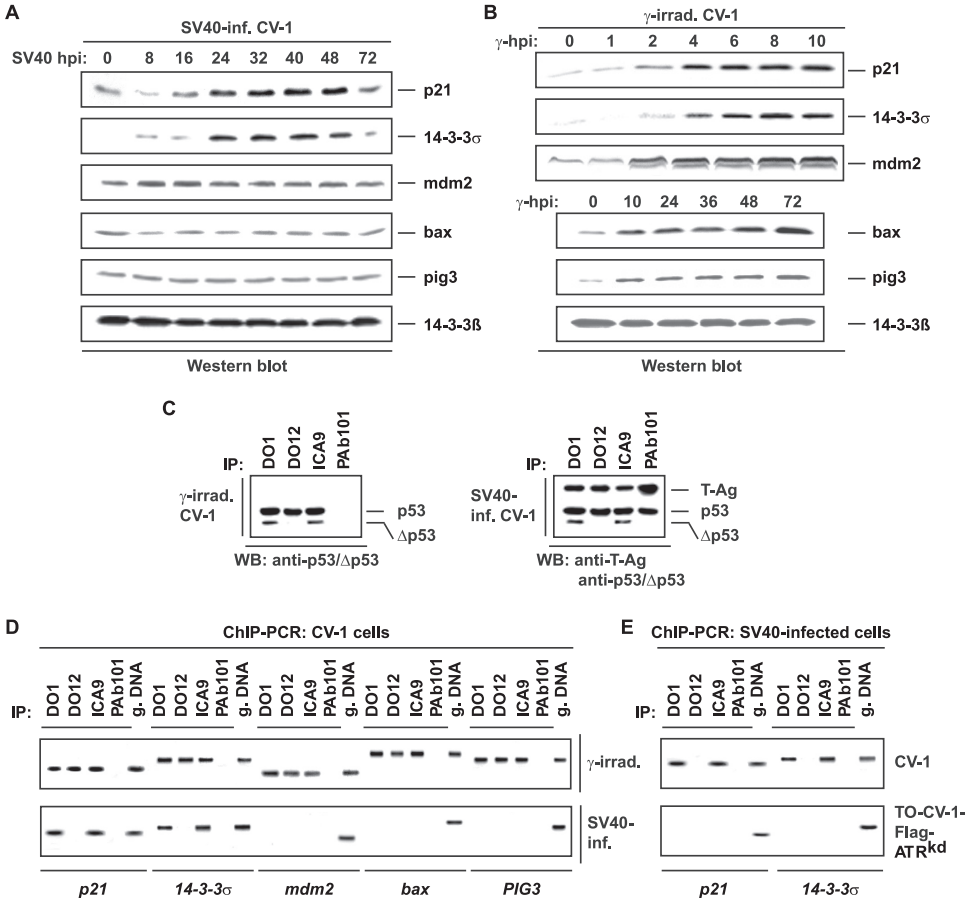

FIG. 4. SV40 infection induces ATR-dependent activation of Δp53. (A and B) SV40-infected (inf.) (A) or γ-irradiated (10 Gy) (γ-irrad.) (B) CV-1 cells were analyzed by immunoblotting for p21, 14-3-3σ, mdm2, bax, and pig3 induction at various times posttreatment; 14-3-3β served as a loading control. (C) γ-Irradiated or SV40-infected CV-1 cells were treated with formaldehyde 8 h or 24 h posttreatment, respectively, and were processed for ChIP. Cross-linked p53/Δp53-DNA complexes were precipitated with anti-p53/Δp53 antibodies DO1 and ICA9 and with anti-p53 antibody DO12. The anti-T-Ag antibody PAb101 served as a negative control. Precipitates were analyzed by immunoblotting (WB) either with the anti-p53/Δp53 antibody SAPU alone or with both SAPU and the anti-T-Ag antibody R9. (D) ChIP-associated *p21*, *14-3-3σ*, *mdm2*, *bax*, and *PIG3* promoter DNAs were identified by PCR. Genomic DNA (g. DNA) served as a marker for the ChIP-PCR products. The ethidium bromide-stained bands represent relative amounts of the promoter DNA recovered by PCR amplification of DNA extracted from precipitates as in panel C. (E) Infected CV-1 and ATR^{kd} cells were treated with formaldehyde 24 hpi and were processed for ChIP. Cross-linked p53/Δp53-DNA complexes were precipitated with antibodies as for panel D. Associated *p21* and *14-3-3σ* promoter DNAs were identified by PCR as for panel D.

promoters. Moreover, ChIP-PCR analysis performed with infected ATR^{kd} cells demonstrated that *p21* and *14-3-3σ* promoter DNAs were not recovered from the immunoprecipitates (Fig. 4E), verifying that ATR is the Δp53-activating kinase.

The specificity of Δp53-mediated upregulation of p21 and 14-3-3σ in infected permissive cells was further investigated in TO-CV-1-Flag-mutΔp53 cells, where Dox-induced expression of ectopic Flag-tagged mutΔp53-R175D inactivates endogenous Δp53 by dominant-negative effects (45). Immunoblot analysis using anti-Flag antibody M2 showed that Flag-mutΔp53 was detectable 8 hpi (Fig. 5A). Reduced stabilization and, accordingly, reduced S-15 phosphorylation of endogenous Δp53 became obvious by comparative Western blot analysis, indicating that ectopically expressed mutΔp53 negatively influences the expression level of endogenous Δp53 (Fig. 5B). However, Flag-mutΔp53 did not interfere with the activation of the ATM and ATR signaling cascades, as evidenced by the appearance of the phosphorylated downstream targets Chk2, p53, T-Ag, and Chk1 (Fig. 5C).

Flag-mutΔp53-mediated inactivation of the transcriptional activity of endogenous Δp53 was demonstrated first by analyzing the expression level of the Δp53-inducible gene products. In infected mutΔp53 cells, no induction of p21 and 14-3-3σ expression, and no upregulation of the p53-inducible gene products mdm2, bax, and pig3, was seen (Fig. 5D). ChIP-PCR performed as described above for infected CV-1 cells verified that ectopic mutΔp53 abrogates the transactivation of *p21* and *14-3-3σ* (Fig. 5E). Taken together, the data demonstrate that Δp53 displays differential transcriptional activity not only in UV-damaged S-phase cells (45) but also in SV40-infected CV-1 cells and that in both scenarios, the activation of Δp53 depends on ATR.

The ATR-Δp53-p21 pathway downregulates AK activity, promoting cell cycle dysregulation. Cells that are UV irradiated at the G_1/S transition activate the ATR-Δp53-p21 path-

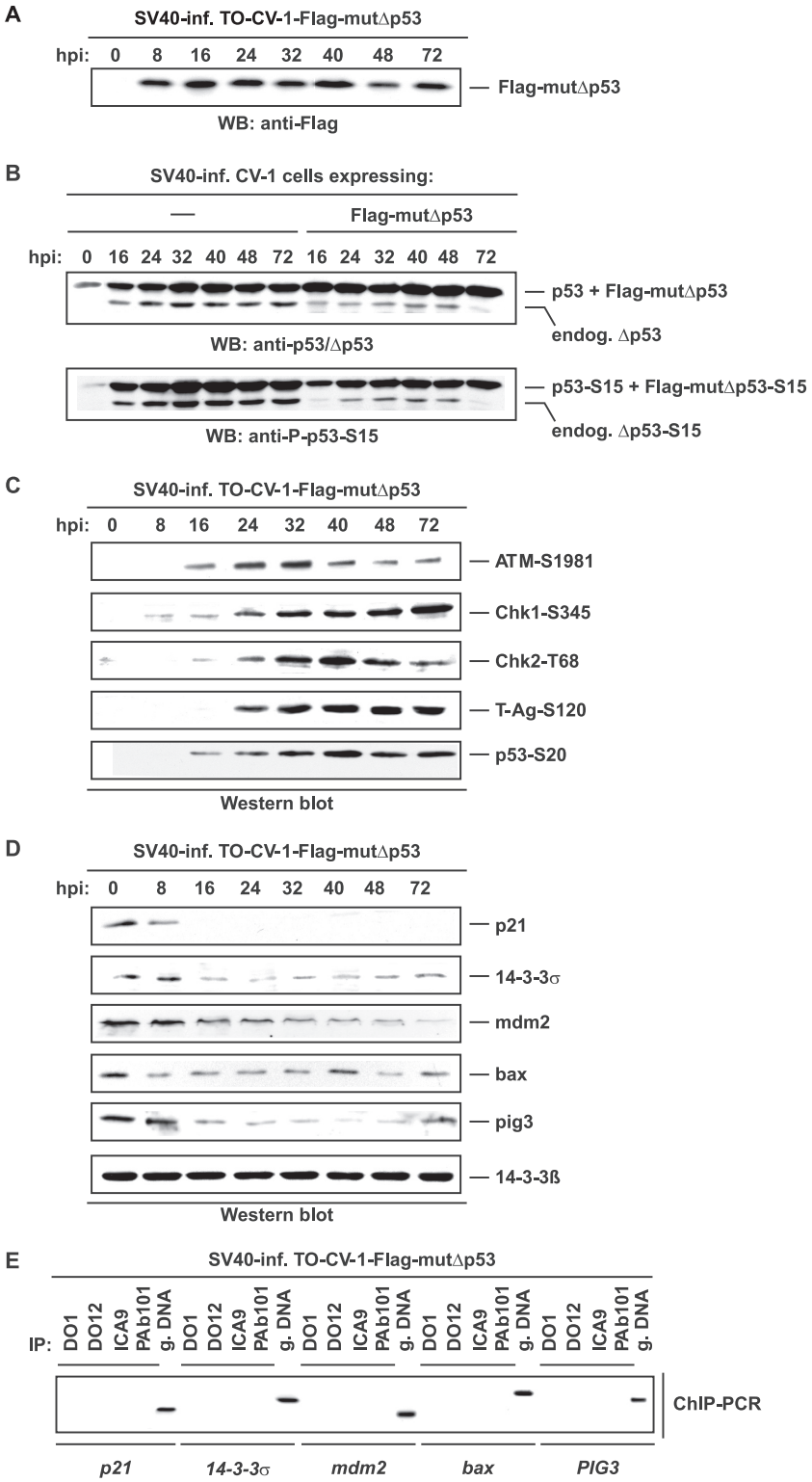

FIG. 5. Ectopically expressed mutΔp53 abrogates the transcriptional activity of endogenous Δp53. (A) Infected (inf.) TO-CV-1-Flag-mutΔp53 cells were analyzed for Dox-induced expression of Flag-mutΔp53 with the anti-Flag antibody M2 at various times postinfection. (B) Lysates prepared from infected CV-1 and mutΔp53 cells at various times postinfection were loaded onto the same sodium dodecyl sulfate gel, transferred to the same membrane, and analyzed for expression and S-15 phosphorylation of p53 and endogenous (endog.) Δp53 by comparative immunoblotting. (C) Immunoblot analysis of phosphorylated ATM, Chk1, Chk2, T-Ag, and p53 in infected mutΔp53 cells. (D) Infected mutΔp53 cells were analyzed by immunoblotting for p21, 14-3-3σ, mdm2, bax, and pig3 induction at different times postinfection; 14-3-3β served as a loading control. (E) Infected mutΔp53 cells were treated with formaldehyde 24 hpi, and the dominant-negative effect of Flag-mutΔp53 was analyzed by ChIP-PCR as for Fig. 4D.

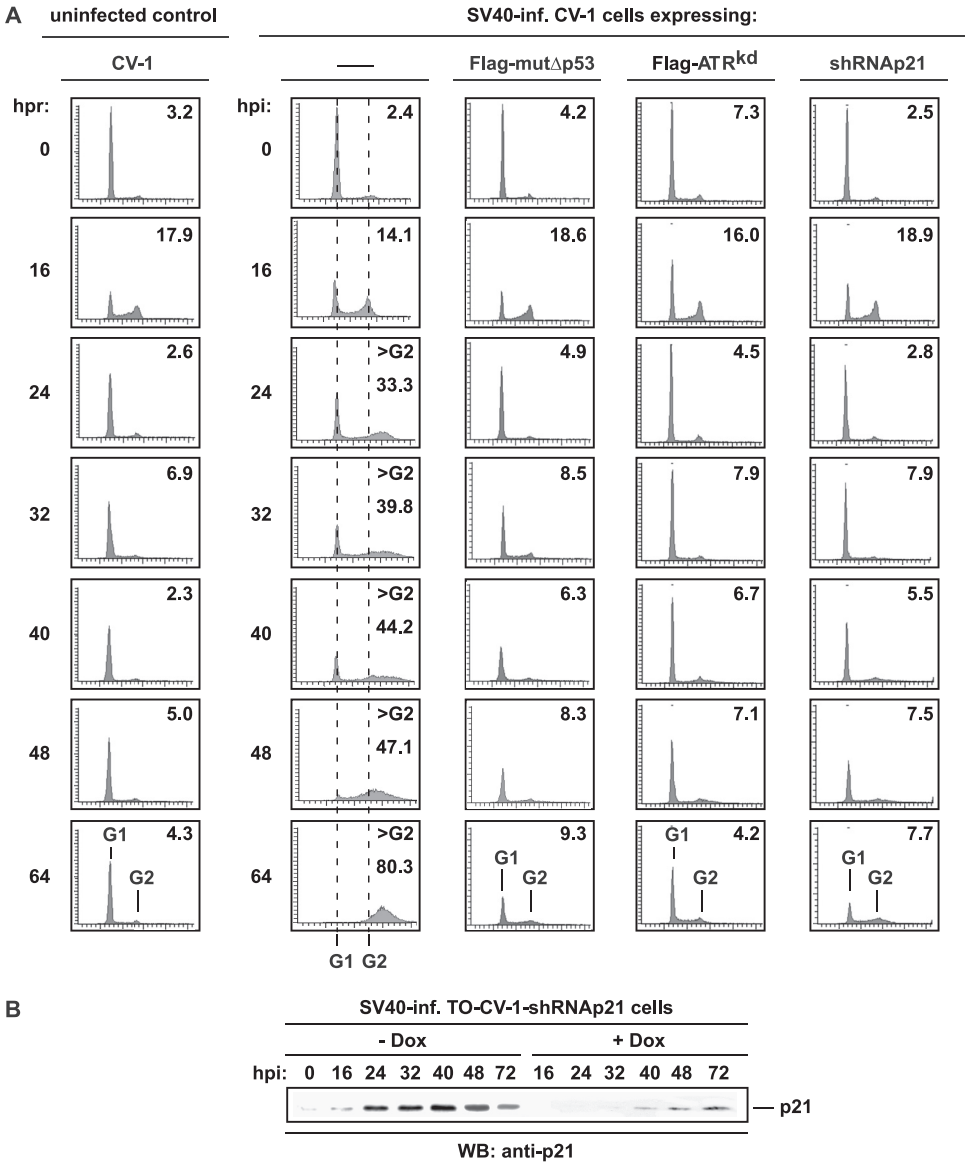

FIG. 6. ATR-Δp53-mediated expression of p21 leads to polyploidization. (A) Pseudo-G_0-arrested CV-1 cells either were released by the addition of complete medium (uninfected control) or were infected with SV40 (—), as were pseudo-G_0-arrested TO-CV-1-Flag-mutΔp53, -ATR^{kd}, and -shRNAp21 cells. Mock-infected and SV40-infected pseudo-G_0 CV-1 cells, as well as infected pseudo-G_0 TO-CV-1-Flag-mutΔp53, -ATR^{kd}, and -shRNAp21 cells, were harvested at the indicated hour postrelease (hpr) or postinfection and were stained with propidium iodide to measure DNA content. The positions of phases G_1 and G_2 are marked, and the percentage of cells in S phase is given in each panel, except for panels marked $>G_2$, where the percentage of infected CV-1 cells with >4N DNA contents is indicated. (B) Parental CV-1 and TO-CV-1-shRNAp21 cells were infected with SV40, and the stable TO-CV-1-shRNAp21 cell line was induced with Dox at 1.5 hpi. Cells were harvested at the indicated time postinfection, and cell extracts were analyzed for p21 expression by comparative immunoblotting (WB).

way, leading to a transient reduction in AK activity and thereby promoting the attenuation of S-phase progression (45). Thus, the physiological implications of ATR-dependent, Δp53-mediated *p21* transactivation for cell cycle progression were investigated in infected CV-1 and TO-CV-1 cells. For better resolution, cells were synchronized in pseudo-G_0 by isoleucine depletion (45) prior to viral infection. Altogether, six samples were collected at various times postinfection until the virus-producing cells indicated a pronounced cytopathic effect (64 hpi). In addition, uninfected CV-1 cells in pseudo-G_0 were examined in order to compare cell cycle events in infected cells to those in cells stimulated with complete medium only. In uninfected as well as infected cells, the FACS profiles showed that cells progressed through S into G_2 at 16 h postrelease or postinfection, respectively, and appeared to progress normally through the first cycle, before cell cycle changes became obvious during the second cycle (Fig. 6A). While the percentage of total cells in S phase remained about the same in uninfected CV-1 cells and infected mutΔp53 and ATR^{kd} cells, the DNA content of infected CV-1 cells increased beyond 4N by 24 hpi, indicating that cells underwent a second and even a third round of DNA replication without mitosis (Fig. 6A). Determi-

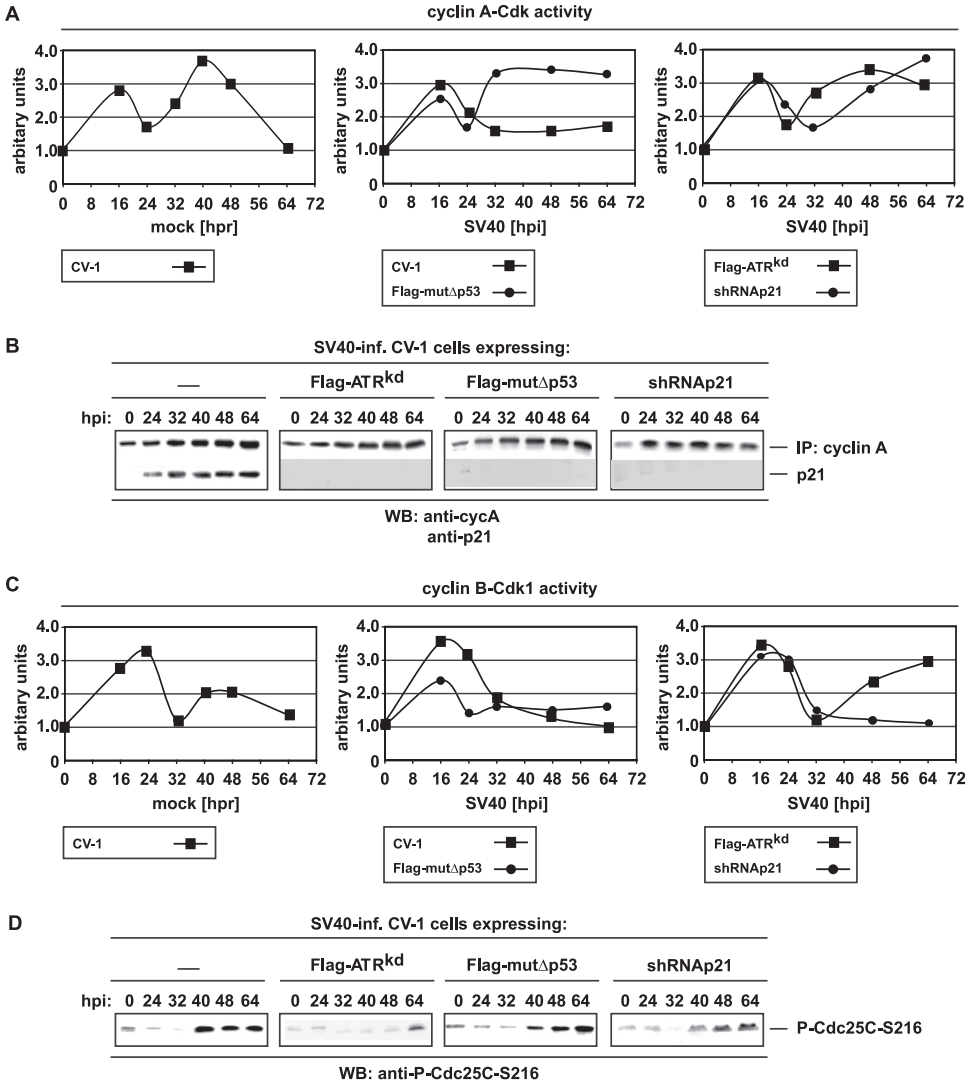

FIG. 7. ATR-Δp53-mediated expression of p21 downregulates AK activity. (A) Pseudo-G_0-arrested CV-1 cells were released by the addition of complete medium (left) or were infected with SV40, as were pseudo-G_0-arrested TO-CV-1-Flag-mutΔp53 cells (center) and TO-CV-1-Flag-ATR^{kd} and TO-CV-1-shRNAp21 cells (right). Mock- and SV40-infected CV-1 cells, as well as infected TO-CV-1-Flag-mutΔp53, -Flag-ATR^{kd}, and -shRNAp21 cells, were harvested at the indicated hour postrelease (hpr) or hour postinfection (hpi) (*x* axis) and were subjected to target-bound AK assays. The relative amount of kinase activity, normalized to the kinase activity measured from cells at 0 h, is shown (*y* axis). (B) Analysis of the association of cycA with p21 in infected (inf.) CV-1, ATR^{kd}, mutΔp53, and shRNAp21 cells by immunoprecipitation (IP) and Western blotting (WB). (C) A target-bound BK1 assay was performed in the same way as the target-bound AK assay for which results are shown in panel A. (D) Immunoblot analysis of infected CV-1, ATR^{kd}, mutΔp53, and shRNAp21 cells for Cdc25C phosphorylation at S-216.

nation of the rate of $a > G_2$ DNA content showed that 80% of infected CV-1 cells had DNA contents of >4N at 64 hpi. Thus, the data confirmed that SV40 lytic infection of permissive cells, such as CV-1, induces the reinitiation of DNA synthesis within a single cell cycle, resulting in the production of polyploid cells (28). Moreover, infected TO-CV-1-shRNAp21 cells, in which Dox-induced expression of shRNAp21 knocks down endogenous p21 at the RNA level (Fig. 6B), also did not acquire a >4N DNA content (Fig. 6A), demonstrating that Δp53-mediated expression of p21 is responsible for cell cycle dysregulation.

The observed virus-induced polyploidization suggests that cell cycle dysregulation involves alteration of the Cdk activity level. Thus, the impact of the Δp53-mediated upregulation of the Cdk inhibitor p21 on AK activity in infected CV-1 cells, as well as in ATR^{kd}-, mutΔp53-, and shRNAp21-expressing TO-CV-1 cells, was examined using a target-bound kinase assay. For the evaluation, synchronized CV-1 and TO-CV-1 cells were infected with SV40 in pseudo-G_0 and were harvested at the indicated times postinfection. Uninfected pseudo-G_0 CV-1 cells served as a control to enable the comparison of Cdk activity obtained from infected cells to that in cells stimulated with complete medium. In all of the cells examined, the AK activity was high at 16 hpi and low at 24 hpi (Fig. 7A), indicating that the cells had completed one mitotic cycle in about 24 h. The uninfected control and infected TO-CV-1 cells entered the next cell cycle after 24 or 32 hpi, as corroborated by the increased AK activity. In the uninfected control, AK

activity dropped after 40 h postrelease and was completely inhibited 64 hpi, indicating that the cells had stopped proceeding through the cell cycle due to growth arrest (Fig. 7A, left). In SV40-infected mutΔp53, ATR^{kd}, and shRNAp21 cells, AK activity remained elevated, although a slight reduction was noticed in mutΔp53 and ATR^{kd} cells 64 hpi (Fig. 7A, center and right), probably due to the more-pronounced cytopathic effect in these cells. In contrast, in SV40-infected CV-1 cells, AK activity continued to decline after 24 hpi, was reduced by 70% at 32 hpi, and was still reduced by 60% at the end of the 64-h observation period (Fig. 7A, center). Thus, the data demonstrate that only in infected CV-1 cells with an intact ATR-Δp53-p21 pathway is substantial downregulation of AK activity observed.

In addition, complex formation between cycA and p21 was evaluated in order to confirm that p21 inhibits AK activity by interaction. Immunoblot analysis showed that p21 was recovered from cycA precipitates starting at 24 hpi (Fig. 7B). Thus, the kinetics of immunoprecipitated cycA-p21 complexes correlated with the observed downregulation of cycA activity in infected CV-1 cells. As expected, in infected, Dox-induced mutΔp53, ATR^{kd}, and shRNAp21 cells, p21 was not recovered from cycA precipitates (Fig. 7B).

Recently, it was suggested that the Chk1-Cdc25C pathway contributes to the inhibition of cyclin B-Cdk1 (BK1) activity in SV40-infected CV-1 cells (37). Since Chk1 is phosphorylated in infected CV-1, mutΔp53, and shRNAp21 cells (data not shown for shRNAp21 cells), but not in ATR^{kd} cells, BK1 activity should not be inhibited in ATR^{kd} cells. In uninfected control cells, BK1 activity displayed the same course as that observed for AK activity, confirming that cells stopped proliferating due to growth arrest (Fig. 7C, left). Measurement of the BK1 activity in infected CV-1 and TO-CV-1 cells showed that at the beginning of the observation period, BK1 presented nearly the same kinetics as those observed for AK (Fig. 7C, center and right). Starting at 32 hpi, BK1 activity was more or less inhibited in CV-1, mutΔp53, and shRNAp21 cells, whereas in ATR^{kd} cells, which are unable to activate Chk1, BK1 activity increased steadily until the end of the 64-h observation time (Fig. 7C, center and right). Evaluation of the phosphorylation status of the Cdk1-activating phosphatase Cdc25C demonstrated that robust phosphorylation of Cdc25C was detectable in infected CV-1, mutΔp53, and shRNAp21 cells but not in ATR^{kd} cells (Fig. 7D), verifying that ATR-activated Chk1 is responsible for Cdc25C and thus for BK1 inactivation. Moreover, the data demonstrate that the Δp53-p21 branch of the ATR-signaling pathway is responsible for AK downregulation but is not involved in the ATR-Chk1-mediated BK1-inactivating step.

The replication efficiency of SV40 depends on the ATR-Δp53-p21 pathway. Optimal production of SV40 progeny requires a nearly continuous S phase, since viral replication depends on the host's replication machinery, which is active only in S. Thus, the ATR-Δp53-p21 pathway, which facilitates the reduction of AK activity and, accordingly, extended attenuation of S-phase progression, should benefit SV40 amplification. In order to investigate this assumption, the replication efficiency of SV40 in the presence or absence of intra-S checkpoint components ATR, Δp53, and p21 was determined. The kinetics of viral replication in infected CV-1, TO-CV-1-Flag-ATR^{kd}, -mutΔp53, and shRNAp21 cells were evaluated by measuring [^{3}H]thymidine incorporation into SV40 DNA. mutΔp53 and shRNAp21 cells exhibited 80% less ^{3}H incorporation than CV-1 cells, whereas in ATR^{kd} cells, the amount of SV40 DNA was reduced below 90% (Fig. 8A). However, inactivation of ATR or Δp53 or knockdown of p21 had no negative impact on the T-Ag expression level, as corroborated by comparative immunoblotting (Fig. 8B), suggesting a correlation between Δp53-mediated downregulation of AK activity and viral replication efficiency.

The impact of functional Δp53 on viral replication efficiency was further evaluated by comparing the replication efficiency in p53/Δp53 knockdown TO-CV-1-TR cells, encoding the tetracycline repressor (TR) only, with that in Δp53-reconstituted TO-CV-1-Flag-wtΔp53 cells. An adenovirus (Ad) vector-mediated, Dox-inducible shRNA expression system for knocking down endogenous p53 and Δp53 was established. First, to examine the efficiency of the Ad vector-mediated shRNAp53 expression system, TR-expressing TO-CV-1-TR cells were infected with various concentrations of Ad-TO-shRNAp53 and were cultured for 3 days before Dox was added to induce shRNAp53 expression. Two days after Dox addition, mock-infected and Ad-infected TO-CV-1-TR cells were UV irradiated for p53/Δp53 stabilization; they were analyzed 6 h postirradiation. Examination of the levels of p53 and Δp53 expression by Western blotting showed that an MOI of 10 efficiently silenced target gene expression (Fig. 8C, lane 4). Next, TO-CV-1 cells expressing ectopic Flag-tagged wtΔp53 upon Dox addition were infected with Ad-TO-shRNAp53 and were cultured for 3 days before Dox was added in order to induce shRNAp53 and Flag-wtΔp53 expression simultaneously. Uninduced Ad-TO-shRNAp53-infected TO-CV-1-Flag-wtΔp53 cells served as a control. After 2 additional days, uninduced or Dox-induced Ad-TO-shRNAp53-infected TO-CV-1-Flag-wtΔp53 cells were infected with SV40, and expression of T-Ag, endogenous p53, and ectopic Flag-wtΔp53 was analyzed by immunoblotting at the indicated times postinfection (Fig. 8D). In addition, approximately 70% of Ad-TO-shRNAp53-infected, Dox-induced TO-CV-1-Flag-wtΔp53 cells expressed ectopic Flag-wtΔp53, as corroborated by immunofluorescence using anti-Flag antibody M2 (data not shown). Expression of Ku80 was also measured as an internal control (Fig. 8D). The results show that T-Ag was expressed in the absence or presence of Dox, whereas probing of the membrane with the anti-p53 antibody DO12, which does not recognize Δp53, demonstrated the silencing effect of the presence of Dox on p53 expression (Fig. 8D). Probing of the membrane with anti-Flag antibody M2 demonstrated that ectopic expression of Flag-wtΔp53 was seen only in Dox-induced, SV40-infected p53/Δp53 knockdown TO-CV-1-Flag-wtΔp53 cells (Fig. 8D).

The impact of Δp53 on cell cycle progression in SV40-infected cells devoid of endogenous p53 was investigated in SV40-infected TO-CV-1-TR and TO-CV-1-Flag-wtΔp53 cells, both of which were exposed to Ad-TO-shRNAp53 and Dox as described above. In the presence of Dox, endogenous p53/Δp53 expression is silenced in both cell lines, whereas expression of Δp53 is restored only in TO-CV-1-Flag-wtΔp53 cells. SV40-induced activation of the transcriptional activity of ectopic Flag-wtΔp53 was confirmed by evaluating the expression level of p21. Western blot analysis demonstrated that p21 was

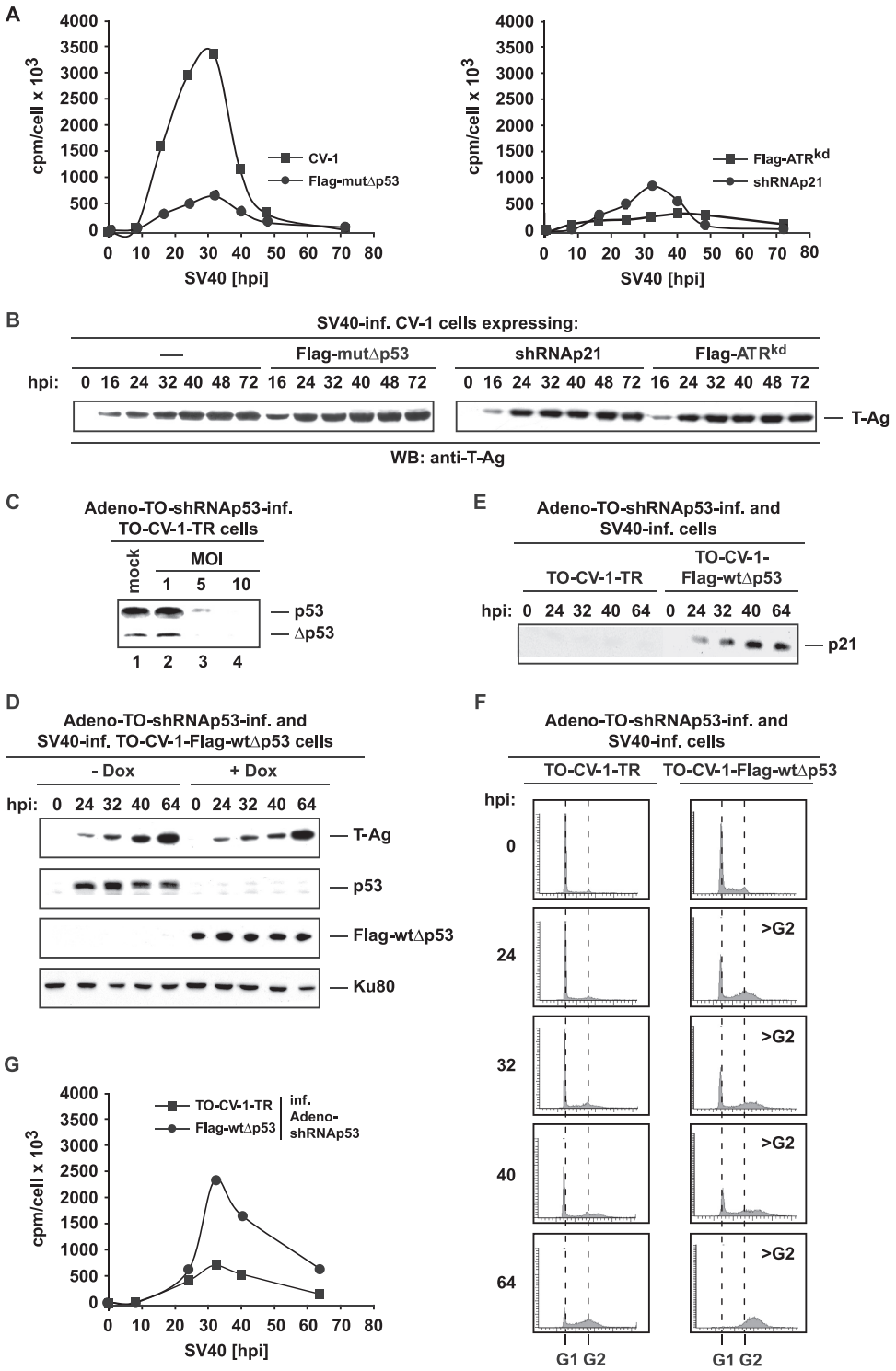

FIG. 8. The ATR-Δp53-p21 pathway is essential for SV40 replication. (A) ^{3}H incorporation was measured in infected CV-1, TO-CV-1-Flag-mutΔp53, ATR^{kd}, and shRNAp21 cells. Cells were labeled with ^{3}H for 60 min at the indicated times after infection (*x* axis). Viral DNA was isolated by the Hirt extraction method, and the resulting ratios of ^{3}H cpm to μg DNA were determined as a measure of DNA synthesis per 1,000 cells (*y* axis). (B) Lysates, prepared from infected (inf.) cells as for panel A at the indicated times postinfection, were loaded onto the same sodium dodecyl sulfate gel, transferred to the same membrane, as indicated, and analyzed for T-Ag expression by comparative immunoblotting (WB) using the anti-T-Ag antibody PAb101. (C) TO-CV-1-TR cells were either mock infected (lane 1) or infected with the Ad-TO-shRNAp53 virus at an MOI of 1, 5, or 10 as indicated (lanes 2 to 4). After 3 days, Dox was added to induce shRNAp53 expression. Cells were then cultured for 2 days, after which they were UV irradiated. At 6 h postirradiation, lysates were prepared for the examination of p53 and Δp53 protein levels by Western blotting using the anti-p53 antibody DO1. (D) TO-CV-1-Flag-wtΔp53 cells were infected with the Ad-TO-shRNAp53 virus, and after 3 days, cells were cultured with or without Dox for 2 additional days prior to SV40 infection. Lysates prepared at various times post-SV40 infection were loaded

detectable only in infected TO-CV-1-Flag-wtΔp53 cells, not in TO-CV-1-TR cells (Fig. 8E). The cell cycle progression of SV40-infected TO-CV-1-TR cells and Flag-mutΔp53-expressing TO-CV-1 cells was determined by FACS analysis at specific times postinfection. The profiles show that no substantial polyploidization was observed in SV40-infected TO-CV-1-TR cells, which are devoid of endogenous p53 and Δp53 (Fig. 8F, left). In contrast, in p53/Δp53 knockdown TO-CV-1-Flag-wtΔp53 cells, where expression of Δp53 was restored upon Dox addition, SV40 infection induced a >4N DNA content starting at 32 hpi (Fig. 8F, right), demonstrating that functional Δp53 plays a major part in the polyploidization process. Next, SV40 replication efficiency in Ad-shRNAp53-infected TO-CV-1-TR and TO-CV-1-Flag-wtΔp53 cells was evaluated by measuring ^{3}H incorporation into SV40 DNA. In contrast to Flag-wtΔp53-expressing TO-CV-1 cells, TO-CV-1-TR cells exhibited an approximately 70% decrease in ^{3}H incorporation (Fig. 8G). Thus, the data clearly show that in p53/Δp53 knockdown TO-CV-1-TR cells, SV40 replication is highly inefficient, but replication efficiency is restored when expression of Δp53 is reconstituted in p53/Δp53 knockdown TO-CV-1-Flag-wtΔp53 cells, revealing Δp53 as a major player in SV40 replication.

Downregulation of AK activity is essential for the maintenance of active viral replication centers. Since the replication efficiency of SV40 is significantly reduced in the presence of high AK activity, it is likely that ATR-Δp53-mediated downregulation of AK activity is essential for establishing active viral replication centers. Accordingly, the formation of T-Ag foci and EdU-incorporating T-Ag foci, which represent prospective and existing active viral replication centers, respectively, in infected CV-1, ATR^{kd}, and mutΔp53 cells was investigated by confocal microscopy at specific times postinfection. For the investigation, an early (24 hpi) and a late (40 hpi) time point were chosen in order to monitor the presence of viral replication factories as a function of time. In all infected cell lines, the formation of T-Ag foci was clearly detectable 24 hpi, demonstrating that the emergence of potential viral replication centers is ATR/Δp53 independent (Fig. 9A, left). Visualization of active viral replication sites by EdU incorporation revealed that infected CV-1 and mutΔp53 cells, but not infected ATR^{kd} cells, displayed active SV40 replication centers 24 hpi (Fig. 9A, left), whereas at 40 hpi, pronounced EdU-positive T-Ag foci were detectable only in CV-1 cells (Fig. 9A, right). These data suggest that ATR is crucial for the activation of SV40 replication, whereas a loss of functional Δp53 terminates SV40 replication prematurely, explaining the low yield of viral DNA obtained (Fig. 8A and G).

Initiation of SV40 replication requires the recruitment of the host replication factor Polα onto the viral origin by direct interaction with the origin-binding protein T-Ag (14). However, only hypo-Polα, not phosphorylated Polα (P-Polα), interacts with T-Ag (13). The two differently phosphorylated Polα subclasses can be distinguished by monoclonal anti-p180 antibodies specific for the 180-kDa subunit of Polα (13). The hypo-Polα is recruited to the origin and is recognized by the anti-p180 antibody HP180-12 (13). In contrast, the anti-p180 antibody SJK132-20 (56) recognizes only P-Polα, which is incompetent for origin binding and synthesizes the primers for the lagging strand of the replication fork (13). Thus, the presence of hypo-Polα in SV40 replication centers was investigated in CV-1, ATR^{kd}, and mutΔp53 cells by confocal microscopy. T-Ag-colocalizing HP180-12-reactive Polα was clearly detectable in CV-1 cells 24 and 40 hpi, and the sizes of T-Ag foci increased at 40 hpi (Fig. 9B, top). However, in infected mutΔp53 cells, hypo-Polα colocalized with T-Ag only at the early time point in the infection cycle, whereas at 40 hpi, the T-Ag-colocalizing HP180-12-reactive Polα signal was significantly reduced (Fig. 9B, bottom). Inactivation of endogenous ATR had no negative impact on the formation of T-Ag foci but reduced the intensity and amount of T-Ag-colocalizing hypo-Polα considerably, and at 40 hpi, HP180-12-reactive Polα was not detectable (Fig. 9B, center). Thus, the data demonstrate that in the presence of high AK activity, the recruitment of T-Ag-interacting hypo-Polα into prospective SV40 replication centers is significantly diminished, explaining the low SV40 replication efficiency in mutΔp53 and ATR^{kd} cells.

Duplication of the SV40 genome involves origin-dependent initiation of replication and primer synthesis for the generation of Okazaki fragments; accordingly, origin-priming hypo-Polα as well as Okazaki-priming P-Polα should be recruited to viral replication centers. Indeed, the SJK132-20-reactive, non-T-Ag-interacting P-Polα subclass was found in active viral replication factories, as evidenced by visualization of the location of SJK132-20-reactive P-Polα in relation to EdU-positive T-Ag foci (Fig. 9C). However, large T-Ag/EdU-colocalizing P-Polα foci were observed only in infected CV-1 cells (Fig. 9C, top); in mutΔp53 and ATR^{kd} cells, levels of P-Polα-containing active viral replication centers were significantly diminished or even absent, respectively (Fig. 9C, bottom and center). Thus, SV40 replication, like mammalian replication, employs two immunologically distinct Polα subclasses: T-Ag-interacting hypo-Polα, for the initiation of origin-dependent replication, and non-T-Ag-interacting P-Polα, for the initiation of Okazaki fragments (13).

Downregulation of AK activity is essential for the generation of T-Ag-interacting hypo-Polα. *In vitro* phosphorylation of Polα by purified AK inhibits the replication activity of the

onto the same sodium dodecyl sulfate gel, transferred to the same membrane, and analyzed for T-Ag, p53, and Flag-wtΔp53 expression by comparative immunoblotting. Ku80 served as a loading control. (E) Ad-TO-shRNAp53-infected, Dox-induced, SV40-infected TO-CV-1-TR and TO-CV-1-Flag-wtΔp53 cells were examined for p21 expression as for panel D. (F) Ad-shRNAp53-infected TO-CV-1-TR and TO-CV-1-Flag-wtΔp53 cells were cultured for 3 days, induced with Dox, and infected with SV40 after 2 additional days. Cells were harvested at the indicated time postinfection and were stained with propidium iodide to measure DNA content. The positions of phases G_1 and G_2 are marked, and the time points at which infected TO-CV-1-Flag-wtΔp53 cells had considerable >4N DNA content (>G_2) are indicated. (G) ^{3}H incorporation was measured in Ad-shRNAp53-infected, Dox-induced TO-CV-1-TR and TO-CV-1-Flag-wtΔp53 cells at specific times post-SV40 infection. Cells were labeled with ^{3}H for 60 min beginning at the indicated times (*x* axis). Viral DNA was isolated by the Hirt extraction method, and the resulting ratios of ^{3}H cpm to μg DNA were determined as a measure of DNA synthesis per 1,000 cells (*y* axis).

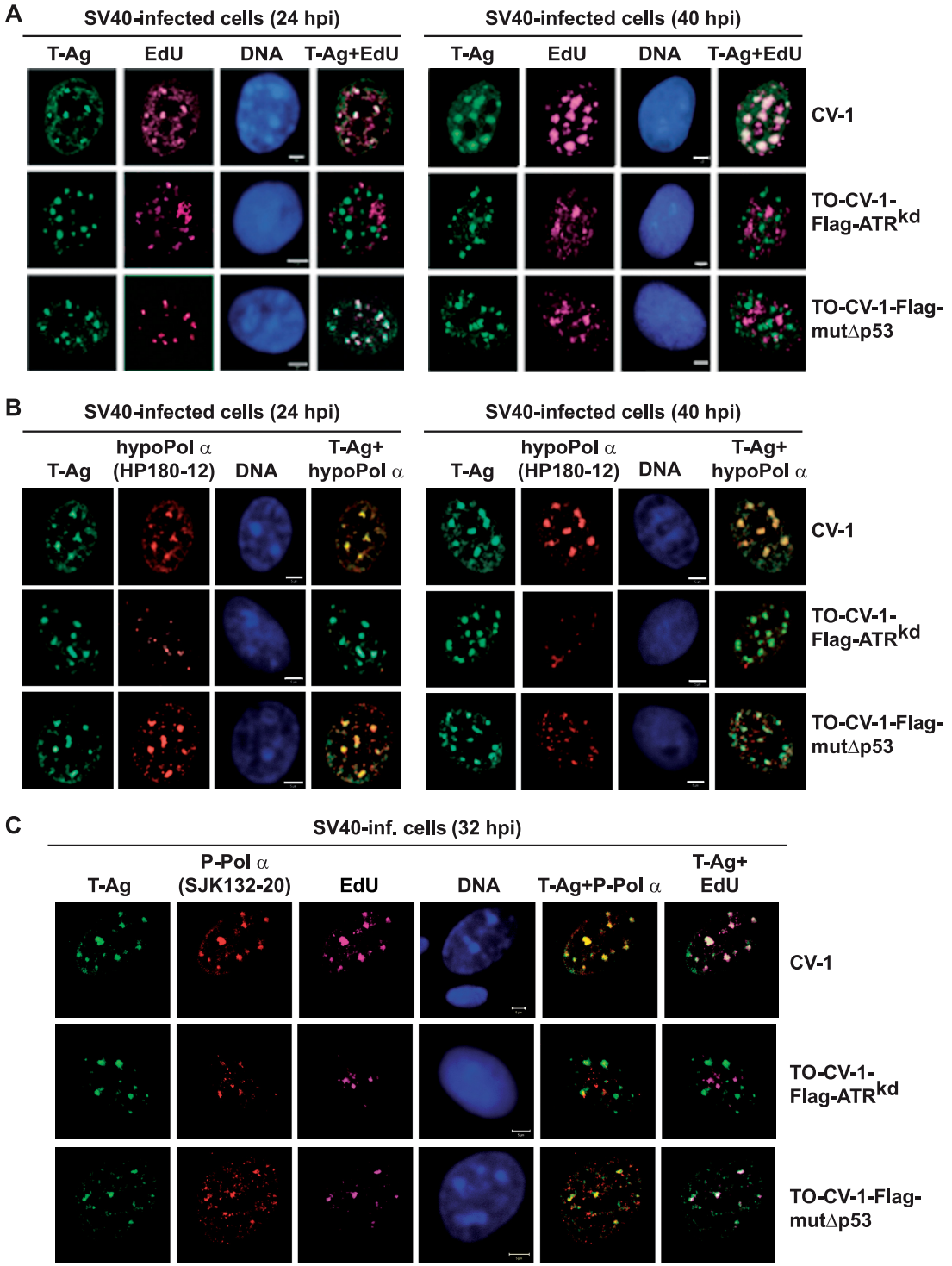

FIG. 9. The ATR-Δp53 pathway is essential for the establishment and maintenance of active SV40 replication centers. (A) For the detection of active DNA replication centers, infected CV-1, ATR^{kd}, and mutΔp53 cells were incubated with EdU 30 min before preextraction, fixed at 24 or 40 hpi, stained, and visualized by confocal microscopy (green, anti-T-Ag antibody R9; magenta, EdU; blue, Hoechst stain). Bars, 5 μm. (B) For the detection of hypo-Polα in SV40 replication centers, infected cells as in panel A were preextracted, fixed at 24 or 40 hpi, stained, and visualized by confocal microscopy (green, anti-T-Ag antibody R9; red, anti-p180 antibody HP180-12; blue, Hoechst stain). Bars, 5 μm. (C) For the detection of P-Polα in SV40 replication centers, infected cells as in panel A were preextracted, fixed at 32 hpi, stained, and visualized by confocal microscopy (green, anti-T-Ag antibody R9; magenta, EdU; red, anti-p180 antibody SJK132-20; blue, Hoechst stain). Bars, 5 μm.

replicase in an SV40 initiation assay, whereas the activities of polymerase α and primase were not impaired in simple enzyme assays (57, 58). The reason for the AK-mediated inhibition of SV40 replication *in vitro* is based on the fact that AK specifically phosphorylates p180 at N-terminal residues T-174, T-219, and S-209 *in vitro* (47), thereby preventing the formation of the Polα–T-Ag complex (13). Since T-219 and S-209 are located within the T-Ag-binding domain C of p180 (Fig. 10A) (14), it is likely that these residues are involved in modulating the T-Ag-binding ability of Polα. Thus, the T-Ag-interacting domain C, which contains two AK sites, and the adjacent noninteracting domain B, which contains all three AK sites (Fig. 10A), were used to verify this assumption. Successful AK2-catalyzed phosphorylation of p180-GST fusion proteins B and C (Fig. 10B, left) was demonstrated by autoradiography (Fig. 10B, right). Nonphosphorylated and AK2-phosphorylated p180 domains B and C (Fig. 10C, left), transferred to a polyvinylidene difluoride (PVDF) membrane, were incubated with T-Ag, and bound T-Ag was detected with the anti-T-Ag antibody PAb101. Far-Western blot analysis confirmed that only p180 domain C, not p180 domain B, interacted with T-Ag, and AK2-phosphorylated p180 domain C demonstrated an inability to bind T-Ag (Fig. 10C, right).

The assumption that the ATR-Δp53-mediated reduction of AK activity is a prerequisite for preventing the conversion of the T-Ag-interacting hypo-Polα into the non-T-Ag-interacting phosphorylated form was further investigated by evaluating the phosphorylation status of p180 in SV40-infected CV-1, mutΔp53, and ATR^{kd} cells at specific times postinfection. Accordingly, a polyclonal anti-p180 antibody exclusively recognizing phosphorylated p180 residue S-209 was generated. The specificity of the anti-P-p180-S209 antibody was analyzed by immunoblotting using bacterially expressed recombinant p180-GST fusion protein 1α (Fig. 10D). The data demonstrate that the phosphospecific anti-p180 antibody recognized only its phosphorylated epitope (Fig. 10E). Before evaluation of the phosphorylation status of p180 in infected CV-1 and mutΔp53 cells, the overall expression level of the 180-kDa Polα subunit was analyzed by comparative immunoblotting. The results obtained with the anti-p180 IgY antibody IDα (14) revealed two polymerase α-reactive bands with molecular masses of 180 (p180) and 165 (*p180) kDa that were clearly detectable starting at 24 hpi and, most strikingly, were observable only in infected CV-1 cells, not in mutΔp53 cells (Fig. 10F, top). Probing of the membrane with an anti-P-p180-S209 antibody demonstrated that in CV-1 cells, phosphorylation of p180 at S-209 was diminished between 24 and 48 hpi, whereas infected mutΔp53 cells displayed large amounts of S-209-phosphorylated p180 (Fig. 10F, bottom). In addition, the anti-P-p180-S209 antibody clearly recognized the 165-kDa polypeptide, demonstrating that S-209-phosphorylated p180 is cleaved only in wtp53 CV-1 cells, not in Δp53-impaired CV-1 cells (Fig. 10F, bottom). In addition, enhanced cleavage of S-209-phosphorylated p180 was not observed in infected ATR^{kd} cells (Fig. 10G). Thus, the data suggest the possibility of selective proteolytic cleavage of S-209-phosphorylated p180 in infected CV-1 cells, which depends on the ATR-Δp53 pathway. This possibility was assessed by treating infected CV-1 cells with the proteasome inhibitor MG132 (44). Lysates obtained from infected CV-1 cells treated with MG132 for 8 h proved that cleavage of S-209-phosphorylated p180 is proteasomal (Fig. 10H, IDα). Probing of the same lysates with the polyclonal anti-p180 antibodies DPN and DPC, specific for the very N and C termini of polymerase α (25), respectively, demonstrated that the 165-kDa *p180 polypeptide results from proteolytic cleavage from the N terminus (Fig. 10H). Consistent with this finding, the steady-state levels of p180 mRNA, determined by Northern blotting, remained steady during the 72-h examination period (Fig. 10I).

These results imply that the cleavage of S-209-phosphorylated p180 and the drop in AK activity decrease the amount of non-T-Ag-interacting P-Polα, giving rise to the T-Ag-interacting hypo-Polα subclass. To validate this assumption, the monoclonal anti-p180 antibodies HP180-12 and SJK132-20, which distinguish between T-Ag-interacting and non-T-Ag-interacting Polα, respectively, were used. Lysates derived from infected CV-1 cells were incubated with monoclonal anti-p180 antibody HP180-12 or SJK132-20, and precipitated Polα was visualized with the N-terminus-specific anti-p180 antibody DPN, which does not distinguish between hypophosphorylated and phosphorylated p180. Immunoblot analysis revealed an increase in the level of HP180-12-reactive p180 between 16 and 40 hpi (Fig. 11A, top left), whereas the level of SJK132-20-reactive p180 was diminished between 16 and 48 hpi (top right). Probing of the HP180-12 and SJK132-20 precipitates with a polyclonal anti-T-Ag antibody demonstrated that only HP180-12-reactive Polα interacted with T-Ag, and the amount of complexed T-Ag correlated with the quantity of precipitated hypo-p180 (Fig. 11A, top). Immunoblot analysis performed with the phosphospecific anti-P-p180-S209 antibody verified that only the SJK132-20-reactive Polα subclass, not the HP180-12-reactive Polα subclass, contains S-209-phosphorylated polymerase α (Fig. 11A, bottom). In addition, immunoblot analysis revealed that large amounts of phosphorylated *p180 were recovered from SJK132-20-precipitated Polα starting at 16 hpi (Fig. 11A, bottom right). In contrast, in infected mutΔp53 cells, the amount of P-p180 was not diminished, and N-terminally cleaved P-p180 was not retrieved from SJK132-20 precipitates, as corroborated by probing of the blots with DPN and anti-P-p180-S209 antisera, respectively (Fig. 11B). Taken together, the data demonstrate that in infected CV-1 cells, P-p180 is mainly N-terminally cleaved, whereas in ATR/Δp53-deficient cells, P-p180 remains predominantly intact.

Since infected mutΔp53 cells, as well as ATR^{kd} cells, failed to downregulate AK activity, it is likely that the amount of T-Ag-interacting hypo-Polα is reduced, thereby limiting the firing of viral origins. Indeed, significantly less HP180-12-reactive Polα was recovered from infected mutΔp53 cells, and in comparison to CV-1 cells, less Polα-complexed T-Ag was observed (Fig. 11C). In view of the fact that the T-Ag levels were not reduced in mutΔp53 cells (Fig. 8B), ruling out the possibility that T-Ag is the viral replication efficiency-limiting aspect, the significant reduction in the level of Polα–T-Ag complex formation in those cells is plausibly caused by the small amount of hypo-Polα. Thus, the SV40-induced AK activity-reducing ATR-Δp53 pathway is essential for the generation of the T-Ag-interacting hypo-Polα subclass, thereby enhancing Polα–T-Ag complex formation and, accordingly, the production of viral progeny. Moreover, the data demonstrate that efficient SV40 replication requires physical contact between

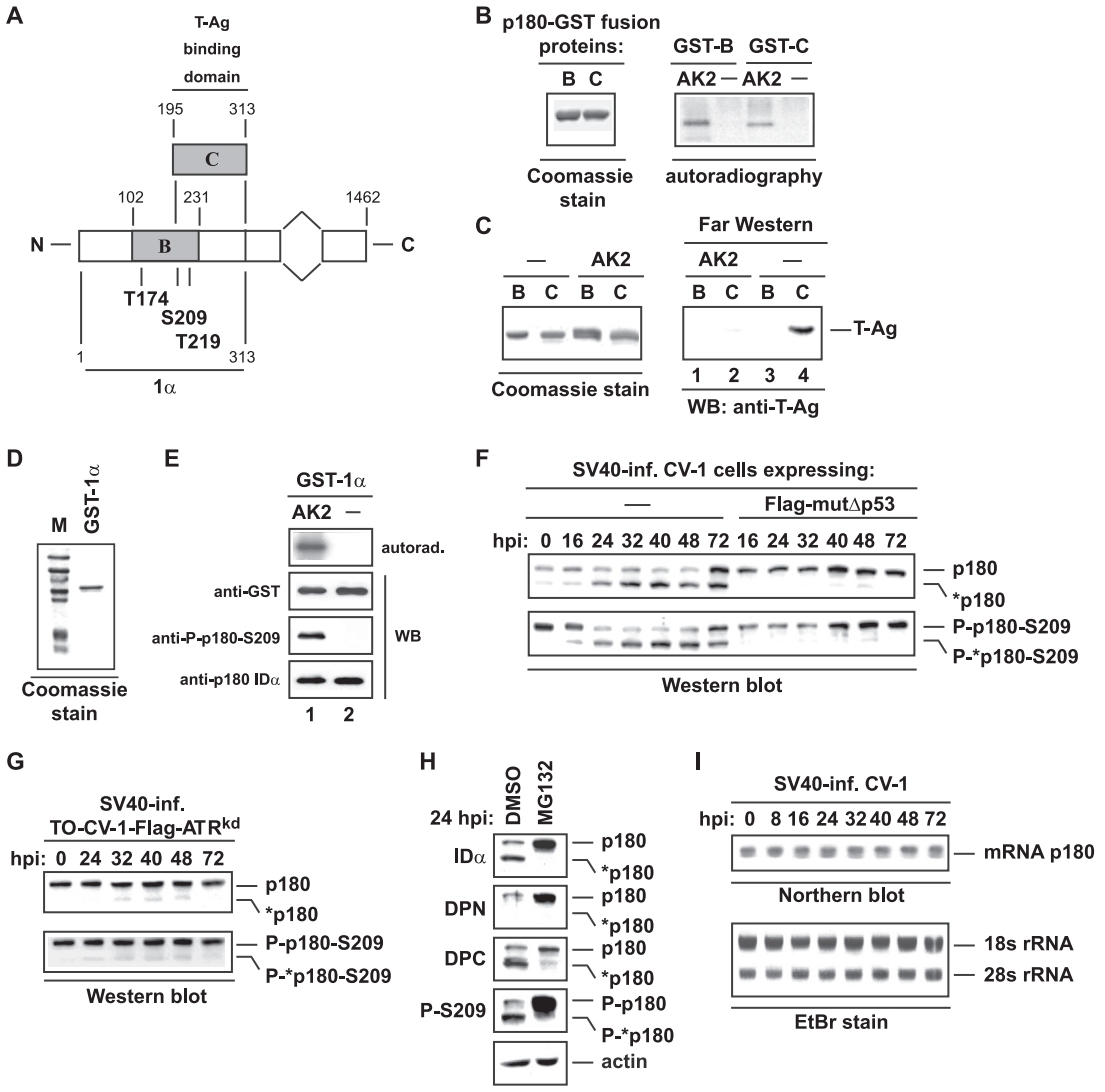

FIG. 10. The ATR-Δp53 pathway diminishes levels of non-T-Ag-interacting AK2-phosphorylated Polα. (A) Schematic representation of p180-GST fusion protein 1α and the two overlapping 1α-GST fusion proteins B and C. The locations of the N-terminal AK phosphorylation sites T-174, S-209, and T-219, and that of the T-Ag-interacting domain C of p180, are indicated. (B) Purified bacterially expressed p180-GST fusion proteins B and C were visualized by Coomassie staining, either left unphosphorylated (—) or phosphorylated by cyclin A-Cdk2 (AK2), and analyzed by autoradiography. (C) Unphosphorylated or AK2-phosphorylated p180-GST fusion proteins B and C were separated on a sodium dodecyl sulfate gel, transferred to a membrane, and incubated with purified recombinant T-Ag. Bound T-Ag was detected with the anti-T-Ag antibody PAb101. WB, Western blotting. (D) Purified bacterially expressed GST-1α protein was resolved by electrophoresis and visualized by Coomassie staining. (E) GST-1α protein was incubated either with purified AK2 and [γ-^{32}P]ATP (AK2) or with kinase-dead AK2^{kd} and [γ-^{32}P]ATP (—) and was analyzed by sodium dodecyl sulfate-polyacrylamide gel electrophoresis and autoradiography (top panel). AK2-phosphorylated and unphosphorylated (—) GST-1α proteins were visualized with an anti-GST antibody (second panel) and were used to analyze the reactivity of the polyclonal anti-P-p180-S209 antibody by immunoblotting (third panel). The polyclonal anti-p180 IgY antibody IDα was used to detect nonphosphorylated and AK2-phosphorylated GST-1α (bottom panel). (F) Lysates prepared from infected CV-1 and mutΔp53 cells at various times postinfection were loaded onto the same sodium dodecyl sulfate gel, transferred to the same membrane, and analyzed for expression and S-209 phosphorylation of p180 by comparative immunoblotting using the anti-p180 antibody IDα and the phosphospecific anti-P-p180-S209 antibody as indicated. *p180 shows 165-kDa N-terminally cleaved P-p180-S209. (G) Lysates prepared from infected, Dox-induced TO-CV-1-ATR^{kd} cells were analyzed for expression and S-209 phosphorylation of p180 as for panel F. (H) SV40-infected CV-1 cells were treated with either 10 μM MG132 or the dimethyl sulfoxide (DMSO) solvent control at 16 hpi. Eight hours later, cell lysates were prepared and analyzed for polymerase α by sodium dodecyl sulfate-polyacrylamide gel electrophoresis and immunoblotting with antisera DPN, DPC, and anti-P-p180-S209, as indicated. p180 and *p180 indicate full-length 180-kDa and N-terminally cleaved 165-kDa polymerase α, respectively. Actin was used as a loading control. (I) Equal amounts of total RNA isolated from infected CV-1 cells at the indicated times postinfection were processed for Northern blot analysis. Equal loading was confirmed by visualizing 18S and 28S rRNA by staining the denatured agarose gel with ethidium bromide (EtBr). The level of Polα subunit p180 RNA was determined with an [α-^{32}P]dCTP-labeled p180 DNA probe.

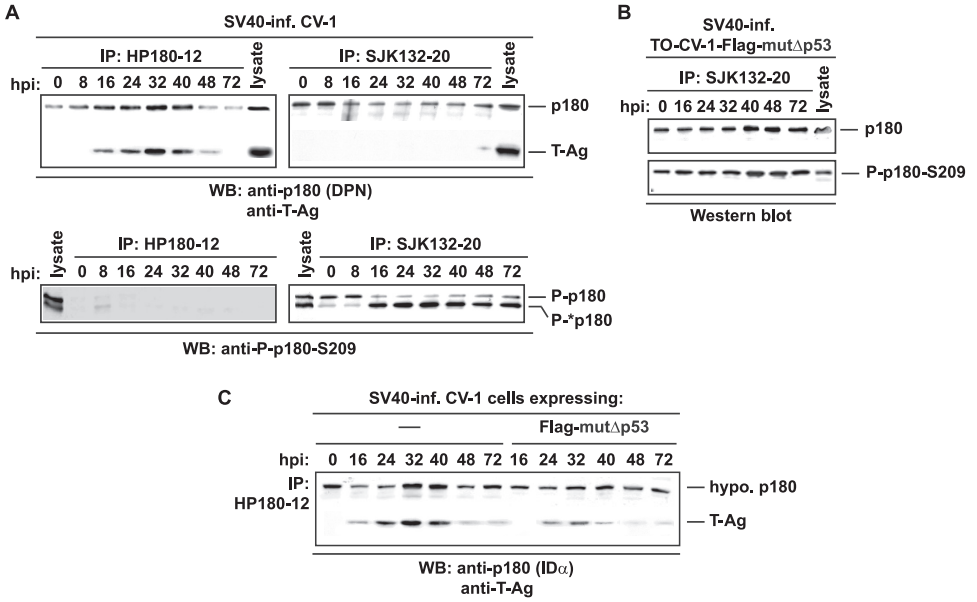

FIG. 11. The ATR-Δp53 pathway enhances T-Ag–Polα complex formation. (A) HP180-12- and SJK132-20-precipitated hypo- and P-Polα, respectively, derived from infected (inf.) CV-1 cells at various times postinfection, were analyzed for associated T-Ag with the anti-T-Ag antibody R9. Precipitated Polα was analyzed for expression and S-209 phosphorylation with the N-terminus-specific anti-p180 antibody DPN and the phosphospecific anti-P-p180-S209 antibody as indicated. *P-p180 shows 165-kDa N-terminally cleaved S-209-phosphorylated p180. WB, Western blotting. (B) SJK132-20-precipitated P-Polα, derived from infected mutΔp53 cells at various times postinfection, was analyzed for expression and S-209 phosphorylation using the anti-p180 antibody IDα and the phosphospecific anti-P-p180-S209 antibody as indicated. (C) HP180-12-precipitated hypo-Polα proteins derived from infected CV-1 and mutΔp53 cells were loaded onto the same sodium dodecyl sulfate gel, transferred to the same membrane, and analyzed by comparative immunoblotting for associated T-Ag with the anti-T-Ag antibody R9. Precipitated hypo-Polα was analyzed for p180 expression with the anti-p180 antibody IDα.

hypo-Polα and T-Ag, revealing hypo-Polα as the rate-limiting step in the production of viral progeny.

DISCUSSION

Viruses gain control over the host to support viral replication by first exploiting and then inactivating specific components of the cellular DNA damage response pathway. An example of this type of method is presented by SV40, where viral infection leads to activation of an ATM-dependent DNA damage response (48), followed by inactivation of certain key proteins of the signaling cascade, such as p53 and the Mre11-Rad50-Nbs1 (MRN) subunits Nbs1 and Mre11 (39, 59, 60). These DNA damage components are inactivated by interaction with virally encoded T-Ag, disrupting cell cycle control to create a physiological environment that is beneficial for viral amplification. Apart from its function as a cell cycle modulator, SV40 T-Ag is an essential viral replication factor that recruits host DNA replication factors to the viral origin (2). Although the molecular basis of SV40 DNA replication has been studied extensively (50), the mechanism underlying the modulation of the host DNA replication machinery supporting viral replication *in vivo* is not fully understood. We show that the *p53* status of the host is important for SV40 amplification. The data demonstrate that in SV40-infected permissive cells, optimal viral DNA replication depends on the transcriptional activity of the novel p53 isoform Δp53, which was first discovered in mammalian cells UV irradiated at the G_1/S transition and operates in the ATR intra-S checkpoint (45).

Our investigations revealed that Δp53, like p53, is stabilized in SV40-infected CV-1 cells but, unlike p53, is not targeted by T-Ag. Since residues 102 to 292 make up the T-Ag-interacting domain of p53 and residues 257 to 322 are nonexistent in Δp53, it is likely that the absent T-Ag-contacting residues 273, 280, and 288 (29) prevent the formation of a complex between Δp53 and T-Ag. Moreover, a 3-dimensional prediction for the structure of Δp53 suggests that a major alpha-helical structure is missing at the C-terminal end, changing the further orientation of the protein, resulting in a more compacted structure (3). Thus, the lack of T-Ag-contacting residues and structural changes explain the inability of Δp53 to interact with T-Ag. Apart from the different 3-dimensional structure, the p53 isoform, in contrast to p53, is refractory to Chk1/2-catalyzed S-20 phosphorylation, since the Chk1/2-docking *BOX-V* motif is missing (11). Furthermore, virally induced stabilization and activation of Δp53 depend strictly on ATR-catalyzed S-15 phosphorylation, whereas phosphorylation of p53 at S-15 is independent of ATR and, unexpectedly, of ATM. The conclusion derived from examining infected cells that were devoid of functional ATM and ATR was confirmed by the abrogated phosphorylation of their downstream targets Chk2 and Chk1. Since DNA-PK has been shown to phosphorylate p53 at S-15 (27), it is likely that in KU-55933-treated ATR^{kd} cells, this PIK kinase is the responsible p53 modifier. Moreover, in ATR/ATM-inactive cells, phosphorylation of ATM at the S-1981 autophosphorylation site was observed, demonstrating that the presence of phosphorylated ATM at residue S-1981 is not a reliable indicator of the kinase's activity status. In view of the fact that ATR-dependent ATM-S1981 phosphorylation was observed in UV-

irradiated cells (52), DNA-PK could phosphorylate ATM at this site as well. This finding suggests that different types of SV40-induced stimuli activate PIK kinases ATM, ATR, and DNA-PK, combining multiple signaling pathways to connect viral DNA replication with the host's repair machinery. Although T-Ag alone is sufficient to activate the ATM/ATR-mediated DNA damage response (22), the detailed molecular mechanisms by which SV40 infection activates the multitargeted ATM/ATR/DNA-PK pathways to modulate the host's physiological environment for its own needs is still not fully understood.

Besides taking advantage of the DNA damage response to promote viral replication by ATM-mediated activation of the replication abilities of T-Ag (48), SV40 has to modulate signaling pathways so as to force the cells to enter S phase and to maintain S phase. The reason for this approach is that SV40 replication depends, with the exception of virally encoded T-Ag, solely on the host's replication factors, such as topoisomerases, replication protein A (RPA), and polymerases α plus δ, factors that are replication competent only in S phase. Thus, optimal production of progeny virus presupposes not only extension of the replicative S phase but also protection of the host's replication machinery activity. DNA replication is tightly regulated by Cdks; while cyclin E-dependent kinase activity is a key player in origin licensing, cyclin A is thought to play a negative role as a licensing inhibitor, ensuring that origins fire only once per cell cycle. Since SV40 infection mobilizes the ATR-Δp53-p21 pathway to reduce S-phase-promoting AK activity by 70%, attenuation of S phase progression and alternation of cellular DNA replication activity can be expected. Indeed, productive SV40 infection overrides the host's once-and-only-once replication cycle, leading to a $>G_2$ DNA content (28). Thus, SV40 stimulates multiple rounds of cellular DNA synthesis, suggesting that changes in the regulators of the cell cycle, such as the Cdks, deregulate replication control, giving rise to tetraploid-polyploid cells. The fact that SV40-induced endoreplication depends on Δp53-mediated downregulation of AK activity was first observed in cells expressing dominant-negative ATR^{kd} or mutΔp53, both of which were deficient in reducing AK activity. Furthermore, knockdown of Δp53-transactivated *p21* or endogenous *p53*/Δ*p53* completely abrogated the polyploidization process; however, restoration of Δp53 and accordingly p21 expression gave rise to a $>G_2$ DNA content. Although previous reports demonstrated that SV40 lytic infection alters cell cycle regulation by Chk1-mediated inhibition of the mitosis-promoting factor (MPF) (37), endoreplication was observed only in infected cells that were able to downregulate AK activity, indicating that the MPF-inhibiting pathway is not triggering polyploidization. Thus, SV40 dysregulates the host's replication control by reducing AK activity, suggesting that the ATR-Δp53-p21 pathway maintains the S-phase environment and replication competence of the host, thereby creating a physiological environment that should be beneficial for viral replication. Indeed, reduction of AK activity correlated with the onset of vigorous viral DNA replication, whereas in infected CV-1 cells that are devoid of the ATR-Δp53-p21 pathway and accordingly are unable to downregulate AK activity, viral amplification was significantly diminished or even repressed. Our data demonstrate that deregulation of AK but not BK1 activity is crucial for SV40 genome amplification, indicating that for SV40 the replication-promoting checkpoint is intra-S and not G_2, in contrast to the human polyomavirus JC virus (JCV), which replicates its genome only in G_2-arrested cells (38). Deregulation of Cdk activity and accordingly cell cycle progression was also observed for mouse polyomavirus, which induces ATM- and ATR-mediated inhibition of AK and BK1 activity, thereby promoting S- and G_2-phase blocks in productively infected cells (12). In contrast to SV40, polyomavirus-infected cells do not acquire $>G_2$ DNA content; accordingly, they display S-phase and not $>G_2$ accumulation. Although mouse polyomavirus is closely related to SV40, differences in the multitargeted activated DNA damage pathways, as well as differences imposed by the unrelated hosts, may explain the contrasting outcomes in cellular replication control. Our results imply that productive SV40 infection does not lead to entry into G_2 and M phases, since high AK activity is required for the transition from S into G_2, and BK1 activity is mandatory for entry into mitosis (19).

The formation of T-Ag foci in SV40-infected cells signifies prospective, existing, or shut-down viral replication factories. Consequently, the amount and continuity of EdU-incorporating T-Ag foci, reflecting active SV40 replication centers, are measures of viral amplification efficiency. Indeed, only in infected CV-1 cells, which are fully capable of enabling the ATR-Δp53-mediated intra-S checkpoint, were active SV40 replication centers observed at early and late times postinfection. Thus, reduction of AK activity correlates with continuously active SV40 replication centers and explains the fact that abrogation of the AK-inhibiting ATR-Δp53-p21 pathway negatively affects viral yield. The reason for the dramatic decrease observed in viral amplification is that in the presence of high AK activity, the initiator of viral replication, host replication factor Polα, is sparsely recruited into prospective viral replication centers. The explanation for this observation is that only hypo-Polα, not AK-phosphorylated Polα, interacts physically and functionally with origin-recruiting T-Ag (13, 47). Moreover, SV40 utilizes the ATR-Δp53-signaling pathway to purposefully diminish levels of the non-T-Ag-interacting Polα subclass by cleaving the S-209-phosphorylated catalytic p180 subunit at its N terminus. Proteolytic cleavage of P-p180 occurs most likely at the specific site between K-123 and K-124 within the RNVKKLAVTKPNN sequence (25), explaining why the 165-kDa *p180 degradation product is recognized by the phosphospecific anti-P-p180-S209 antibody. However, the ATR-Δp53 signaling-dependent molecular mechanisms, causing proteasomal degradation of P-p180, remain to be elucidated. Thus, the potential benefit to SV40 replication of activating the intra-S checkpoint is to keep the host's replication machinery initiation competent by preventing the AK-catalyzed inactivation of origin-competent hypo-Polα and by reducing the amount of non-T-Ag-interacting P-Polα. In addition, the results could partially explain the continued replication of host cell chromosomal DNA beyond 4N in SV40-infected permissive cells (28). The premise of firing an origin of replication once and only once could be overruled in SV40-infected cells, since the AK activity level might not be high enough to inactivate origin-licensing factors, allowing hypo-Polα-catalyzed reinitiation of licensed origins. On the other hand, the finding does not quite explain how the host cell replication machinery stays active in the presence of the ATR-mediated intra-S

checkpoint, which has been shown to be responsible for extended DNA replication inhibition in UV-damaged S-phase cells (45). One possible explanation could be that the host's replication activity could be rescued by cyclin E-Cdk2, since cyclin E expression and its associated activity were significantly increased in SV40-infected permissive cells (data not shown). In view of the fact that overexpression of cyclin E or cyclin A or irregular activity of these Cdk complexes leads to genomic instability in mammalian cells (9, 51), it is likely that the ATR-Δp53-p21-mediated deregulation of AK activity sets off the polyploidization process in SV40-infected permissive cells.

As shown previously, expression of p21 stimulates endoreplication, but only in retinoblastoma protein (pRb)-negative cells (35), indicating that pRb is an important factor in the cellular response to p21-mediated downregulation of Cdk activity. Together with the transcription factor E2F, which activates genes required for S phase, such as those encoding cyclins A and E (36), pRb controls the oscillatory dynamics of the Cdk network, thereby ensuring the successive phases of the cell cycle. Cdk-catalyzed phosphorylation of pRb releases E2F, whereas dephosphorylation of pRb leads to the sequestration and inactivation of E2F. In UV-irradiated as well as SV40-infected CV-1 cells, dephosphorylation and consequently activation of pRb were observed, events that correlated with the onset of the ATR-Δp53-p21-mediated downregulation of AK activity (data not shown). However, in SV40-infected cells, T-Ag binds and inactivates hypophosphorylated pRb (31), disrupting the balance between the antagonistic effects of E2F and pRb, which promote or delay cell cycle progression, respectively. Thus, T-Ag-mediated neutralization of the inhibitory functions of pRb negatively influences the ATR-Δp53-p21-mediated intra-S checkpoint by enabling transcription of E2F-regulated genes, many of which encode proteins required for DNA replication, repair, and nucleotide metabolism. In addition, T-Ag targets Nbs1, a cellular factor that is thought to participate in the control of DNA replication initiation in the intra-S checkpoint by preventing additional reinitiation of origins that have already fired (59). The rereplication suppression function of Nbs1 is inhibited following T-Ag–Nbs1 complex formation, leading both to enhancement of SV40 DNA replication initiation and to endoreplication of chromosomal DNA (59). Taking the data together, we suggest that SV40 overrides the intra-S checkpoint through the effects of T-Ag on the cellular checkpoint factors pRb and Nbs1, thereby promoting endoreplication via the ATR-Δp53-p21-mediated downregulation of AK activity, which might be sufficient to allow the initiation of replication but not sufficient to prevent reinitiation.

In contrast to the situation in SV40-infected permissive cells, AK and BK1 activities are rapidly elevated upon T-Ag expression in nonpermissive and semipermissive mammalian cells, disrupting mitotic control and accordingly genome stability by promoting aneuploidy (8). The discrepancy in Cdk activity levels between productively SV40 infected permissive cells and T-Ag-expressing nonpermissive or semipermissive cells indicates that the mechanisms leading to disruption of the cell cycle and DNA replication control differ. Indeed, in T-Ag-expressing nonpermissive or semipermissive cells, entry into and exit from mitosis are impaired, whereas in productively SV40 infected permissive cells, activation of the intra-S and G_2 checkpoints disrupts S-phase progression. Moreover, T-Ag-mediated transformation is observed only in cells that fail to support SV40 replication, indicating that productive viral infection and ectopic expression of T-Ag do not activate exactly the same signaling networks. Previously it was shown that the process of infection by SV40 and the entry of its genome begin by binding via viral coat protein VP1 to GM1 receptors at the surfaces of the permissive host's cells, leading to activation of the Akt-1 signaling cascade before T-Ag is expressed (7). Thus, SV40 infection induces T-Ag-independent as well as T-Ag-dependent signal transduction pathways, both of which could counteract the T-Ag-mediated transformation process in permissive cells. However, the virally induced cytopathic effect could eliminate all cells on the route toward transformation before they have reached the end. Nevertheless, the question of whether cellular endoreplication is a prerequisite for optimal amplification of the SV40 genome or just a by-product still remains to be addressed.

Although SV40 has to defy the potential inhibitory effects on replication of the ATM and ATR signal transduction pathways, both checkpoint activators are pivotal for viral progeny, since inactivation of ATM or ATR almost completely blocks viral replication. ATM is the major kinase responsible for phosphorylating T-Ag on S-120 *in vivo*, thereby activating the replicative functions of T-Ag (48), whereas ATR is required for preventing the conversion of T-Ag-interacting hypo-Polα into the non-T-Ag-interacting phosphorylated form. Taken together, SV40 utilizes the ATR-Δp53-mediated intra-S checkpoint for two purposes: first, to maintain the host in the S-phase environment, which is optimal for viral amplification, and second, to promote viral amplification by enhancing the T-Ag-interacting, hypo-Polα subpopulation, which is indispensable for origin-dependent replication initiation.

ACKNOWLEDGMENTS

We are grateful to Teresa Wang for DPN and DPC antisera and to Jim Alwine for the GST-T1 construct. The rabbit polyclonal anti-T-Ag antibody R9 was a generous gift from Wolfgang Deppert. Rudolph Reimers graciously helped us with the confocal microscopy. We thank Peter Groitl for technical advice on recombinant adenovirus production and MOI determination.

The financial support of the Deutsche Forschungsgemeinschaft (DO 424/3-1) is appreciatively acknowledged. The Heinrich-Pette-Institute is financially supported by Freie und Hansestadt Hamburg and the Bundesministerium für Gesundheit.

REFERENCES

1. **Alexandrow, M. G., and J. L. Hamlin.** 2004. Cdc6 chromatin affinity is unaffected by serine-54 phosphorylation, S-phase progression, and overexpression of cyclin A. Mol. Cell. Biol. **24:**1614–1627.
2. **Ali, S. H., and J. A. DeCaprio.** 2001. Cellular transformation by SV40 large T antigen: interaction with host proteins. Semin. Cancer Biol. **11:**15–23.
3. **Baumbusch, L. O., S. Myhre, S. A. Langerod, A. Bergamaschi, S. B. Geisler, P. E. Lonning, W. Deppert, I. Dornreiter, and A. L. Borresen-Dale.** 2006. Expression of full-length p53 and its isoform Δp53 in breast carcinomas in relation to mutation status and clinical parameters. Mol. Cancer **5:**47.
4. **Bell, S. P., and A. Dutta.** 2002. DNA replication in eukaryotic cells. Annu. Rev. Biochem. **71:**333–374.
5. **Borowiec, J. A., F. B. Dean, P. A. Bullock, and J. Hurwitz.** 1990. Binding and unwinding—how T antigen engages the SV40 origin of DNA replication. Cell **60:**181–184.
6. **Bullock, P. A., S. Tevosian, C. Jones, and D. Denis.** 1994. Mapping initiation sites for simian virus 40 DNA synthesis events in vitro. Mol. Cell. Biol. **14:**5043–5055.
7. **Butin-Israeli, V., N. Drayman, and A. Oppenheim.** 2010. Host-virus interactions: SV40 infection triggers a balanced network that includes apoptotic, survival, and stress pathways. J. Virol. **84:**3431–3442.

8. **Chang, H.-T., F. A. Ray, D. A. Thompson, and R. Schlegel.** 1997. Disregulation of mitotic checkpoints and regulatory proteins following acute expression of SV40 large T antigen in diploid human cells. Oncogene **14:**2383–2393.
9. **Chibazakura, T., S. G. McGrew, J. A. Cooper, H. Yoshikawa, and J. M. Roberts.** 2004. Regulation of cyclin-dependent kinase activity during mitotic exit and maintenance of genome stability by p21, p27, and p107. Proc. Natl. Acad. Sci. U. S. A. **101:**4465–4470.
10. **Chomczynski, P., and N. Sacchi.** 1987. Single-step method of RNA isolation by acid guanidinium thiocyanate-phenol-chloroform extraction. Anal. Biochem. **162:**156–159.
11. **Craig, A. L., J. A. Chrystal, J. A. Fraser, N. Sphyris, Y. Lin, B. J. Harrison, M. T. Scott, I. Dornreiter, and T. R. Hupp.** 2007. The MDM2 ubiquitination signal in the DNA-binding domain of p53 forms a docking site for calcium calmodulin kinase superfamily members. Mol. Cell. Biol. **27:**3542–3555.
12. **Dahl, J., J. You, and T. L. Benjamin.** 2005. Induction and utilization of an ATM signaling pathway by polyomaviurs. J. Virol. **79:**13007–13017.
13. **Dehde, S., G. Rohaly, O. Schub, H. P. Nasheuer, W. Bohn, J. Chemnitz, W. Deppert, and I. Dornreiter.** 2001. Two immunologically distinct human DNA polymerase alpha-primase subpopulations are involved in cellular DNA replication. Mol. Cell. Biol. **21:**2581–2593.
14. **Dornreiter, I., W. C. Copeland, and T. S. Wang.** 1993. Initiation of simian virus 40 DNA replication requires the interaction of a specific domain of human DNA polymerase alpha with large T antigen. Mol. Cell. Biol. **13:**809–820.
15. **Dornreiter, I., L. F. Erdile, I. U. Gilbert, D. von Winkler, T. J. Kelly, and E. Fanning.** 1992. Interaction of DNA polymerase alpha-primase with cellular replication protein A and SV40 T antigen. EMBO J. **11:**769–776.
16. **Dornreiter, I., A. Hoss, A. K. Arthur, and F. Fanning.** 1990. SV40 T antigen binds directly to the large subunit of purified DNA polymerase alpha. EMBO J. **9:**3329–3336.
17. **Eki, T., T. Matsumoto, Y. Murakami, and J. Hurwitz.** 1992. The replication of DNA containing the simian virus 40 origin by the monopolymerase and dipolymerase systems. J. Biol. Chem. **267:**7284–7294.
18. **Geng, Y., Y. M. Lee, M. Welcker, J. Swanger, A. Zagozdzon, J. D. Winer, J. M. Roberts, P. Kaldis, B. E. Clurman, and P. Sicinski.** 2007. Kinase-independent function of cyclin E. Mol. Cell **25:**127–139.
19. **Graña, X., and E. P. Reddy.** 1995. Cell cycle control in mammalian cells: roles of cyclins, cyclin dependent kinases, growth suppressor genes and cyclin-dependent kinase inhibitors. Oncogene **11:**211–219.
20. **Gruda, M. C., J. M. Zabolotny, J. H. Xiao, I. Davidson, and J. C. Alwine.** 1993. Transcriptional activation by simian virus 40 large T antigen: interactions with multiple components of the transcription complex. Mol. Cell. Biol. **13:**961–969.
21. **Gurney, E. G., R. O. Harrison, and J. Fenno.** 1980. Monoclonal antibodies against simian virus 40 T antigens: evidence for distinct subclasses of large T antigen and for similarities among nonviral T antigens. J. Virol. **34:**752–763.
22. **Hein, J., S. Boichuk, J. Wu, Y. Cheng, R. Freire, P. S. Jat, T. M. Roberts, and O. V. Gjoerup.** 2009. Simian virus 40 large T antigen disrupts genomic integrity and activates a DNA damage response via Bub1 binding. J. Virol. **83:**117–127.
23. **Hickson, I., Y. Zhao, C. J. Richardson, S. J. Green, N. M. B. Martin, A. I. Orr, P. M. Reaper, S. P. Jackson, N. J. Curtin, and G. C. M. Smith.** 2004. Identification and characterization of a novel and specific inhibitor of the ataxia-telangiectasia mutated kinase ATM. Cancer Res. **64:**9152–9159.
24. **Hirt, B.** 1967. Selective extraction of polyoma DNA from infected mouse cell cultures. J. Mol. Biol. **26:**365–369.
25. **Hsi, K. L., W. C. Copeland, and T. S. F. Wang.** 1990. Human DNA polymerase α catalytic polypeptide binds ConA and RCA and contains a specific labile site in the N-terminus. Nucleic Acids Res. **18:**6231–6237.
26. **Ishimi, Y., and Y. Komamura-Kohno.** 2001. Phosphorylation of Mcm4 at specific sites by cyclin-dependent kinase leads to loss of Mcm4,6,7 helicase activity. J. Biol. Chem. **276:**34428–34433.
27. **Lees-Miller, S. P., K. Sakaguchi, S. Ullrich, E. Appella, and C. W. Anderson.** 1992. The human DNA-activated protein kinase phosphorylates serines 15 and 37 in the amino-terminal transactivation domain of human p53. Mol. Cell. Biol. **12:**5041–5049.
28. **Lehman, J. M., J. Laffin, and T. D. Friedrich.** 2000. Simian virus 40 induces multiple S phases with the majority of viral DNA replication in the G_2 and second S phase in CV-1 cells. Exp. Cell Res. **258:**215–222.
29. **Lilyestrom, W., M. G. Klein, R. Zhang, A. Joachimiak, and X. S. Chen.** 2006. Crystal structure of SV40 large T-antigen bound to p53: interplay between a viral oncoprotein and a cellular tumor suppressor. Genes Dev. **20:**2373–2382.
30. **Liu, E., X. Li, F. Yan, Q. Zhao, and X. Wu.** 2004. Cyclin-dependent kinases phosphorylate human Cdt1 and induce its degradation. J. Biol. Chem. **279:**17283–17288.
31. **Ludlow, J. W., J. A. DeCaprio, C. M. Huang, W. H. Lee, E. Paucha, and D. M. Livingston.** 1989. SV40 large T antigen binds preferentially to an underphosphorylated member of the retinoblastoma susceptibility gene product family. Cell **56:**57–65.
32. **Méndez, J., and B. Stillman.** 2000. Chromatin association of human origin recognition complex, cdc6, and minichromosome maintenance proteins during the cell cycle: assembly of prereplication complexes in late mitosis. Mol. Cell. Biol. **20:**8602–8612.
33. **Méndez, J., X. H. Zou-Yang, S. Y. Kim, M. Hidaka, W. P. Tansey, and B. Stillman.** 2002. Human origin recognition complex large subunit is degraded by ubiquitin-mediated proteolysis after initiation of DNA replication. Mol. Cell **9:**481–491.
34. **Mimura, S., and H. Takisawa.** 1998. Xenopus Cdc45-dependent loading of DNA polymerase alpha onto chromatin under the control of S-phase Cdk. EMBO J. **17:**5699–5707.
35. **Niculescu, A. B., III, X. Chen, M. Smeets, L. Hengst, C. Prives, and S. I. Reed.** 1998. Effects of $p21^{Cip1/Waf1}$ at the G_1/S and the G_2/M cell cycle transitions: pRb is a critical determinant in blocking DNA replication and in preventing endoreduplication. Mol. Cell. Biol. **18:**629–643.
36. **Ohtani, K., J. DeGregori, and J. R. Nevins.** 1995. Regulation of the cyclin E gene by transcription factor E2F1. Proc. Natl. Acad. Sci. U. S. A. **92:**12146–12150.
37. **Okubo, E., J. M. Lehman, and T. D. Friedrich.** 2003. Negative regulation of mitotic promoting factor by the checkpoint kinase chk1 in simian virus 40 lytic infection. J. Virol. **77:**1257–1267.
38. **Orba, Y., T. Suzuki, Y. Makino, K. Kubota, S. Tanaka, T. Kimura, and H. Sawa.** 2010. Large T antigen promotes JC virus replication in G_2-arrested cells by inducing ATM- and ATR-mediated G_2 checkpoint signaling. J. Biol. Chem. **285:**1544–1554.
39. **O'Shea, C. C.** 2005. DNA tumor viruses—-the spies who lyse us. Curr. Opin. Genet. Dev. **15:**18–26.
40. **Petersen, B. O., J. Lukas, C. S. Sorensen, J. Bartek, and K. Helin.** 1999. Phosphorylation of mammalian CDC6 by cyclin A/CDK2 regulates its subcellular localization. EMBO J. **18:**396–410.
41. **Pipas, J. M., and A. J. Levine.** 2001. Role of T antigen interactions with p53 in tumorigenesis. Semin. Cancer Biol. **11:**23–30.
42. **Pombo, A., D. A. Jackson, M. Hollinshead, Z. Wang, R. G. Roeder, and P. R. Cook.** 1999. Regional specialization in human nuclei: visualization of discrete sites of transcription by RNA polymerase III. EMBO J. **18:**2241–2253.
43. **Prives, C.** 1990. The replication functions of SV40 T antigen are regulated by phosphorylation. Cell **61:**735–738.
44. **Rock, K. L., C. Gramm, L. Rothstein, K. Clark, R. Stein, L. Dick, D. Hwang, and A. I. Goldberg.** 1994. Inhibitors of the proteasome block the degradation of most cell proteins and the generation of peptides presented on MHC class I molecules. Cell **78:**761–771.
45. **Rohaly, G., J. Chemnitz, S. Dehde, A. M. Nunez, J. Heukeshoven, W. Deppert, and I. Dornreiter.** 2005. A novel human p53 isoform is an essential element of the ATR-intra-S phase checkpoint. Cell **122:**21–32.
46. **Salic, A., and T. J. Mitchison.** 2008. A chemical method for fast and sensitive detection of DNA synthesis in vivo. Proc. Natl. Acad. Sci. U. S. A. **105:**2415–2420.
47. **Schub, O., G. Rohaly, R. W. Smith, A. Schneider, S. Dehde, I. Dornreiter, and H. P. Nasheuer.** 2001. Multiple phosphorylation sites of DNA polymerase alpha-primase cooperate to regulate the initiation of DNA replication in vitro. J. Biol. Chem. **276:**38076–38083.
48. **Shi, Y., G. E. Dodson, S. Shaikh, K. Rundell, and R. S. Tibbetts.** 2005. Ataxia-telangiectasia-mutated (ATM) is a T-antigen kinase that controls SV40 viral replication in vivo. J. Biol. Chem. **280:**40195–40200.
49. **Shiloh, Y.** 2001. ATM and ATR: network cellular response to DNA damage. Curr. Opin. Genet. Dev. **11:**71–77.
50. **Simmons, D. T.** 2000. SV40 large T antigen functions in DNA replication and transformation. Adv. Virus Res. **55:**75–134.
51. **Spruck, C. H., K. A. Won, and S. I. Reed.** 1999. Deregulated cyclin E induces chromosome instability. Nature **401:**297–300.
52. **Stiff, T., S. A. Walker, K. Cerosaletti, A. A. Goodarzi, E. Petermann, P. Concannon, M. O'Driscoll, and P. A. Jeggo.** 2006. ATR-dependent phosphorylation and activation of ATM in response to UV treatment or replication fork stalling. EMBO J. **25:**5775–5782.
53. **Stillman, B.** 1989. Initiation of eukaryotic DNA replication in vitro. Annu. Rev. Cell Biol. **5:**197–245.
54. **Sullivan, C. S., A. T. Grundhoff, S. Tevethia, J. M. Pipas, and D. Ganem.** 2005. SV40-encoded microRNAs regulate viral gene expression and reduce susceptibility to cytotoxic T cells. Nature **435:**682–686.
55. **Takisawa, H., S. Mimura, and Y. Kubota.** 2000. Eukaryotic DNA replication: from pre-replication complex to initiation complex. Curr. Opin. Cell Biol. **12:**690–696.
56. **Tanaka, S., S. Z. Hu, T. S. Wang, and D. Korn.** 1982. Preparation and preliminary characterization of monoclonal antibodies against human DNA polymerase alpha. J. Biol. Chem. **257:**8386–8390.
57. **Voitenleitner, C., E. Fanning, and H. P. Nasheuer.** 1997. Phosphorylation of DNA polymerase alpha-primase by cyclin A-dependent kinases regulates initiation of DNA replication in vitro. Oncogene **14:**1611–1615.
58. **Voitenleitner, C., C. Rehfuess, M. Hilmes, L. O'Rear, P. C. Liao, D. A. Gage, R. Ott, H. P. Nasheuer, and E. Fanning.** 1999. Cell cycle-dependent regulation of human DNA polymerase alpha-primase activity by phosphorylation. Mol. Cell. Biol. **19:**646–656.
59. **Wu, X., D. Avni, T. Chiba, F. Yan, Q. Zhao, Y. Lin, H. Heng, and D.**

Livingston. 2004. SV40 T antigen interacts with Nbs1 to disrupt DNA replication control. Genes Dev. **18:**1305–1316.
60. **Zhao, X., R. J. Madden-Fuentes, B. X. Lou, J. M. Pipas, J. Gerhardt, C. J. Rigell, and E. Fanning.** 2008. Ataxia telangiectasia-mutated damage-signaling kinase- and proteasome-dependent destruction of Mre11-Rad50-Nbs1 subunits in simian virus 40-infected primate cells. J. Virol. **82:**5316–5328.
61. **Zhu, W., C. Ukomadu, S. Jha, T. Senga, S. K. Dhar, J. A. Wohlschlegel, L. K. Nutt, S. Kornbluth, and A. Dutta.** 2007. Mcm10 and And-1/CTF4 recruit DNA polymerase alpha to chromatin for initiation of DNA replication. Genes Dev. **21:**2288–2299.
62. **Zlotkin, T., G. Kaufmann, Y. Jiang, M. Y. Lee, L. Uitto, J. Syvaoja, I. Dornreiter, E. Fanning, and T. Nethanel.** 1996. DNA polymerase epsilon may be dispensable for SV40- but not cellular-DNA replication. EMBO J. **15:**2298–2305.